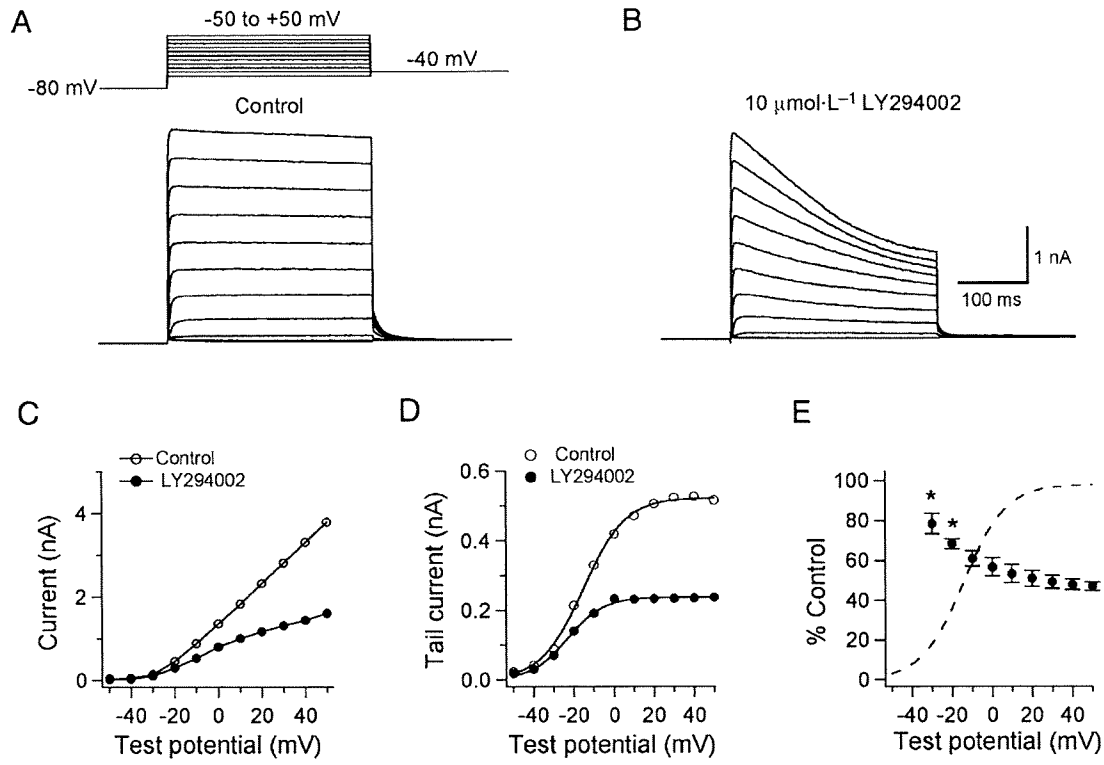

Figure 1 Inhibitory action of LY294002 on human Kv1.5 channels heterologously expressed in a Chinese hamster ovary cell. (A and B) Superimposed human Kv1.5 channel currents elicited during 300 ms depolarizing steps given from a holding potential of −80 mV to potentials between −50 and +50 mV in 10 mV increments, followed by a 200 ms repolarization step to −40 mV before (A, Control) and 3 min after exposure to 10 μmol·L^{-1} LY294002 (B). (C) *I–V* relationships for late currents measured at the end of test steps in control and during exposure to 10 μmol·L^{-1} LY294002. The solid lines were drawn by eye. (D) *I–V* relationships for tail currents in control and during exposure to 10 μmol·L^{-1} LY294002. The smooth curves through the data points represent the least-squares fit to a Boltzmann equation, and the derived $V_{1/2}$ was −14.2 mV in control and −23.2 mV in the presence of LY294002, while *k* was 10.6 mV in control and 8.9 mV in the presence of the compound. The data shown in panels C and D were obtained from the records in panels A and B. (E) Late current amplitude in the presence of LY294002 is plotted as a percentage of control amplitude in the absence of the compound (% Control, filled circles). Data points represent mean ± s.e.mean of six different cells. The dashed curve represents the activation curve obtained in control conditions (see Figure 1D). **P* < 0.05 compared with the values at +50 mV.

response relationship for the inhibition of hKv1.5 current by LY294002, measured at the end of the depolarizing step to +30 mV in seven different cells. The mean data were reasonably well fitted with a Hill equation with an IC_{50} of 7.9 ± 0.5 μmol·L^{-1} and n_H of 1.3 ± 0.2 ($n = 7$).

LY294002 also caused a concentration-dependent acceleration of hKv1.5 current decay during the depolarizing step (to +30 mV). The time constant (τ_D) of block development was measured by fitting a single exponential function to the current trace in the presence of each concentration of LY294002. However, current decay in the presence of lower concentrations (1 and 5 μmol·L^{-1}) of LY294002 was too small to obtain meaningful fits. We therefore omitted the time constant values obtained at low concentrations (1 and 5 μmol·L^{-1}). In Figure 2C, τ_D (measured at +30 mV) was plotted against concentration of LY294002, and data points were fitted to a hyperbolic equation ($\tau_D = 1/(k_{+1}[D] + k_{-1})$), yielding apparent binding (k_{+1}) and unbinding (k_{-1}) rate constants that averaged 1.6 μmol·L^{-1-1}·s^{-1} and 5.7 s^{-1} respectively. The theoretical K_D value derived by k_{-1}/k_{+1} was 3.6 μmol·L^{-1}, which is reasonably close to the value for IC_{50} (7.9 μmol·L^{-1}) derived from a Hill fit of the concentration–response relationship (Figure 2B). This correlation between K_D and IC_{50} may support the hypothesis that LY294002 binds preferentially to hKv1.5 channels in the open state.

Reversible inhibition of hKv1.5 by LY294002

The reversibility of the effect of LY294002 on hKv1.5 current was examined by applying the drug over several consecutive cycles. Figure 3 shows a representative time course of changes in amplitude of hKv1.5 current measured during 300 ms depolarizing step to +30 mV when 10 μmol·L^{-1} LY294002 was applied three times. The hKv1.5 current started to be inhibited within approximately 10 s by each exposure to LY294002, and the steady-state effect (approximately 70% inhibition) was attained about 60 s after the application. The inhibitory effect of LY294002 on hKv1.5 current was fully reversed within approximately 40 s following superfusion with drug-free bath solution. LY294002 was thus found to be a rapidly reversible blocker of the hKv1.5 channel.

We also examined the effect of LY294002 on the deactivation kinetics of the hKv1.5 current. Deactivation time constants, measured by fitting a single exponential function to

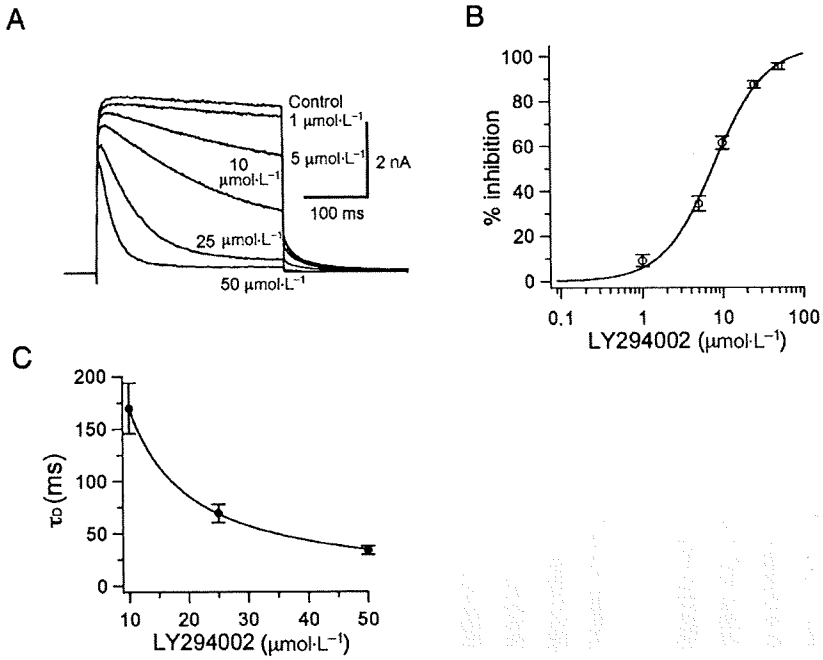

Figure 2 Concentration-dependent block of human Kv1.5 (hKv1.5) current by LY294002. (A) Superimposed hKv1.5 current traces evoked by 300 ms depolarizing step from a holding potential of −80 to +30 mV, followed by a 200 ms repolarization step to −40 mV before (Control) and during exposure to various concentrations (1, 5, 10, 25 and 50 μmol·L^{-1}) of LY294002. (B) Concentration–response relationship for the inhibition of hKv1.5 current by LY294002. Percentage inhibition (% inhibition) represents the fraction of hKv1.5 current reduced by each concentration of LY294002 with reference to the control amplitude, measured at the end of 300 ms depolarizing step to +30 mV. The smooth curve through the data points (mean ± s.e.mean of seven different cells) represents a least-squares fit of a Hill equation, yielding an IC_{50} of 7.9 ± 0.5 μmol·L^{-1} and a Hill coefficient of 1.3 ± 0.2 ($n = 7$). (C) Kinetics of LY294002 block of hKv1.5 current. LY294002-induced time constant at +30 mV was plotted as a function of the drug concentration (10, 25 and 50 μmol·L^{-1}). Note that control hKv1.5 current exhibited no appreciable decay during 300 ms depolarization to +30 mV. The solid line represents the fit of the data to the hyperbolic function (see text).

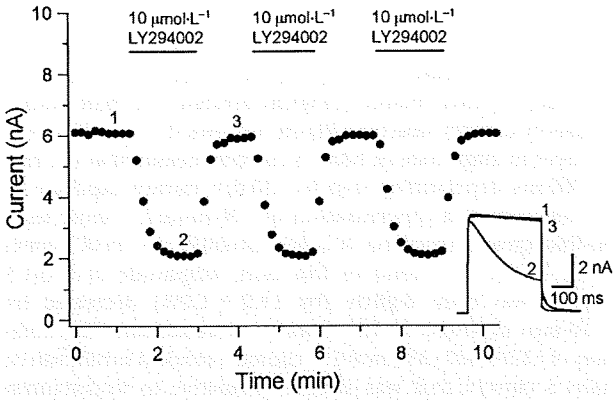

Figure 3 Reversible inhibition of human Kv1.5 (hKv1.5) current by LY294002. The hKv1.5 current was repetitively activated every 10 s by 300 ms depolarizing step to +30 mV from a holding potential of −80 mV, followed by a 200 ms repolarization step to −40 mV. The amplitude of hKv1.5 current measured at the end of the depolarizing step was plotted as a function of time for the entire experiment. LY294002 at a concentration of 10 μmol·L^{-1} was added to the bath during the period indicated by the horizontal bar. The inset illustrates the original current traces recorded at time points indicated by numerals on the graph.

the outward tail current at −40 mV (data not shown, see current traces in the inset of Figure 3) before and during exposure to LY294002, respectively, averaged 11.7 ± 0.82 and 10.7 ± 0.75 ms ($n = 7$, $P > 0.05$), indicating that the deactivation process was not appreciably influenced by this compound.

Frequency-dependent inhibition of hKv1.5 by LY294002

To evaluate whether LY294002 displayed any frequency-dependent effects on hKv1.5 current, trains of 20 depolarizing steps of 300 ms duration from −80 to +50 mV were applied at two different frequencies, 1 and 2 Hz, in the absence and presence of LY294002. The cell was equilibrated in LY294002 for 3 min at −80 mV to keep the channels in the closed state, so that the first sweep represents the first channel opening in the presence of the compound. For the comparison, the control cell was also held at −80 mV for 3 min before applying test pulses. Figure 4A shows superimposed current traces of hKv1.5 recorded during application of such pulse train at a frequency of 2 Hz in the absence (Control) and presence of 10 μmol·L^{-1} LY294002. Under control conditions, the peak current amplitude at the twentieth depolarizing step was reduced by 17.1 ± 1.4% ($n = 7$) at 1 Hz and 33.9 ± 1.6% ($n = 7$) at 2 Hz, compared with the first pulse (Figure 4B). Such a decline may reflect the accumulation of the slow inactiva-

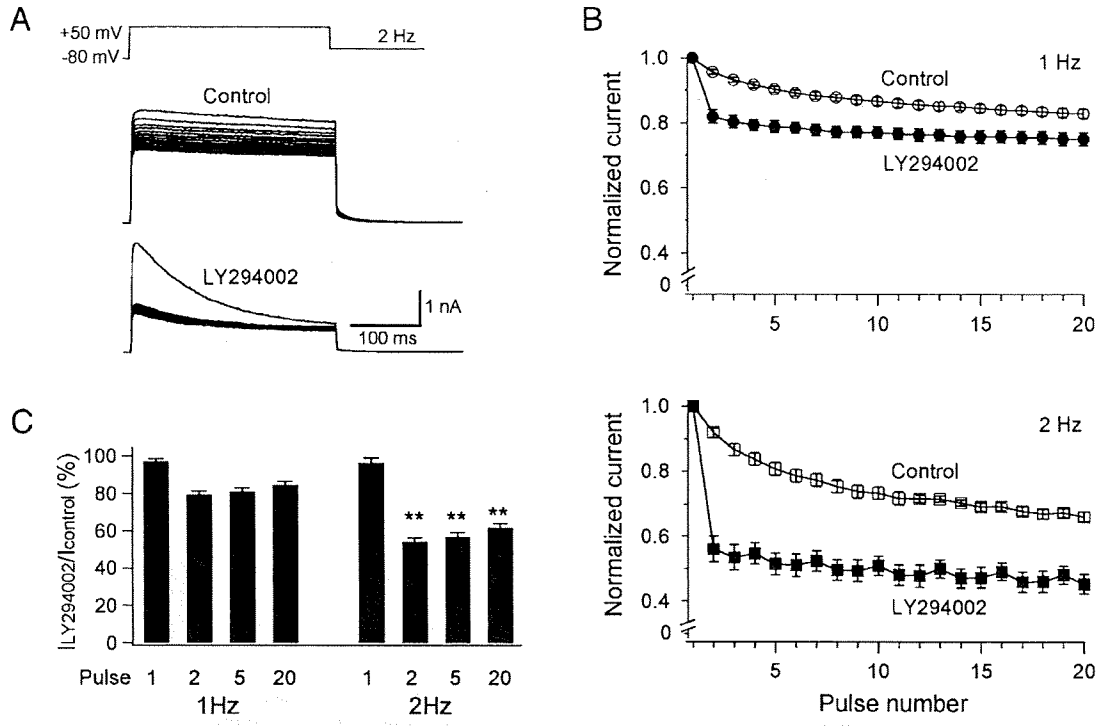

Figure 4 Frequency-dependent inhibition of human Kv1.5 current evoked by LY294002. Human Kv1.5 channels were subjected to 20 repetitive 300 ms depolarizing steps to +50 mV, from a holding potential of −80 mV at frequencies of 1 and 2 Hz, under control conditions and in the presence of 10 μmol·L^{-1} LY294002. (A) Original current traces recorded by application of a train of depolarizing steps at a frequency of 2 Hz under control conditions (upper panel) and after 3 min exposure to 10 μmol·L^{-1} LY294002 (lower panel). (B) Peak amplitudes of outward current at every pulse were normalized with reference to the peak amplitude of current obtained at the first pulse and then plotted against the pulse numbers. Data points represent mean ± s.e.mean ($n = 7$ for each frequency). (C) Normalized current amplitudes in the presence and absence of the drug measured for pulse numbers 1, 2, 5 and 20 at the two frequencies. $^{**}P < 0.01$ compared with that at 1 Hz.

tion of hKv1.5 channels. In the presence of 10 μmol·L^{-1} LY294002, the peak current amplitude at the first depolarizing step was not significantly modified (Figure 4A; control: 4.5 ± 0.8 nA; LY294002: 4.4 ± 0.7 nA, $n = 7$, $P = 0.19$), indicating the absence of tonic block. However, the peak amplitude of hKv1.5 current thereafter progressively decreased by 24.1 ± 1.8% ($n = 7$) and 54.6 ± 3.0% ($n = 7$) at twentieth depolarizing steps at 1 and 2 Hz respectively (Figure 4B). To determine the frequency-dependent effect of LY294002 without contamination of current decline observed under control conditions, the normalized current amplitudes ($I_{LY294002}/I_{control}$) were measured for pulse numbers 1, 2, 5 and 20 at the two frequencies (Figure 4C). These normalized current amplitudes were significantly less at 2 Hz (right hand graph) than the corresponding values at 1 Hz (left hand graph) for pulse numbers 2, 5 and 20. Thus, the degree of inhibition of hKv1.5 increased as the pulse frequency increased, showing that LY294002 blocks hKv1.5 channels in a frequency-dependent manner.

Effects of wortmannin and LY303511 on hKv1.5

PI3K is an important intracellular signalling enzyme that catalyses phosphorylation of phosphatidylinositols and affects a wide range of cellular functions, including growth, migration and survival (Knight *et al.*, 2004). It has also been shown that PI3K is involved in the up-regulation of Kv1 channels by insulin-like growth factor-1 (IGF-1) in HEK (human embryonic kidney) 293 cells (Gamper *et al.*, 2002). We tested whether the inhibition of hKv1.5 current by LY294002 is mediated through PI3K inhibition, using wortmannin, another pharmacological inhibitor of PI3K with a markedly distinct structure. Figure 5 shows the time-course of changes in amplitude of hKv1.5 current measured at the end of 300 ms depolarizing step to +30 mV during exposure to wortmannin at a concentration of 100 nmol·L^{-1}, more than 50-fold greater than the IC_{50} for inhibition of PI3K (Powis *et al.*, 1994). In a total of five cells, amplitude of hKv1.5 current was only slightly (by 11.2 ± 1.0%) decreased by 5–10 min exposure to 100 nmol·L^{-1} wortmannin. The addition of LY294002 (25 μmol·L^{-1}) caused a marked inhibition of hKv1.5 current that was almost insensitive to wortmannin (100 nmol·L^{-1}). These results indicate that inhibition of PI3K was not primarily involved in the LY294002-induced reduction of hKv1.5 current.

We also checked the effect of LY303511, a structural analogue of LY294002, on hKv1.5 current. LY303511 contains a piperazine ring instead of the morpholine ring of LY294002 (Figure 6B) and has no effect on PI3K activity (Ding *et al.*, 1995; Kristof *et al.*, 2005). As shown in Figure 6A, LY303511 at 25 μmol·L^{-1} produced little effect on hKv1.5 current, which was in contrast with a marked inhibition evoked by subsequent application of LY294002 on the same cell. As judged from the structural differences between LY294002 and

LY303511 (Figure 6B), the morpholino oxygen in LY294002 may play a functional role in inhibiting the hKv1.5 currents.

Inhibitory effects of LY294002 on mutant hKv1.5 channels

Recent studies have found that several amino acid residues located in the pore (outer pore or pore helix) and in the S6 domain of hKv1.5 channels provide critical structural components for blockade of the channel by drugs (Decher *et al.*, 2004; 2006; Herrera *et al.*, 2005; Rezazadeh *et al.*, 2006). To investigate possible binding sites of LY294002 to the hKv1.5 channel, nine residues located in the pore and S6 domain were mutated by site-directed mutagenesis. These mutants are T462C and H463C located in the outer mouth of S5-pore linker, T480A located at the base of the pore helix, R487V located in the outer pore region and A501V, I502A, I508A, L510A and V516A located in the S6 domain. As has been reported (Decher *et al.*, 2006; Rezazadeh *et al.*, 2006), all these mutant channels can produce substantial outward currents during depolarization. Figure 7A demonstrates representative examples for the effect of LY294002 (25 μmol·L^{-1}) on WT and three mutant channels (H463C, R487V and I508A) activated during 300 ms depolarizing step to +30 mV from a holding potential of −80 mV. The kinetic properties of both the H463C and the R487V mutant channels appeared to be qualitatively similar to WT, whereas the I508A mutant channel exhibited slower channel kinetics compared with WT channels. Figure 7B summarizes the inhibitory effect of LY294002 (25 μmol·L^{-1}) on WT and various mutant channels, measured as percentage inhibition of late currents at the end of 300 ms depolarizing step (to +30 mV). Whereas the T462C, H463C and A501V channels were inhibited by LY294002 (25 μmol·L^{-1}) to an extent similar to WT, the inhibitory effect of LY294002 (25 μmol·L^{-1}) was significantly less in the T480A, R487V, I502A, I508A, L510A and V516A mutant channels. We also determined the concentration–response relationships for the inhibition of the R487V mutant channel by LY294002 (Figure 7C), yielding an IC_{50} of 16.5 ± 3.6 μmol·L^{-1} (n = 5) for the R487V mutant and 7.9 ± 0.5 μmol·L^{-1} for WT (n = 7, see also Figure 2B). These results indicate that Thr480 at the base of the pore helix, Arg487 in the outer pore region and Ile502, Ile508, Leu510 and Val516 in the S6 domain are important for the block by LY294002.

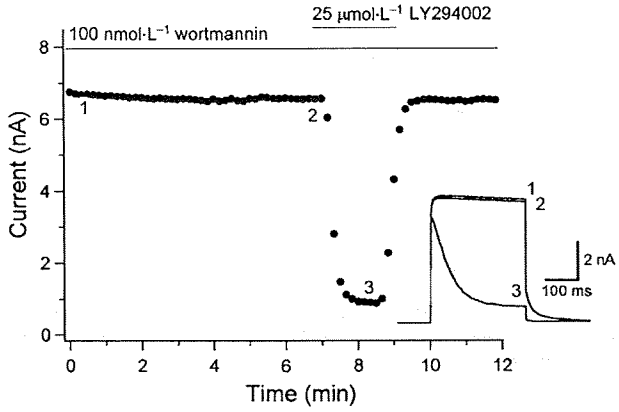

Figure 5 Effect of wortmannin on human Kv1.5 current. The human Kv1.5 current was repetitively (every 10 s) activated with 300 ms depolarizing step to +30 mV from a holding potential of −80 mV, followed by a 200 ms repolarization step to −40 mV and current amplitude measured at the end of depolarizing step was plotted. Inset shows the superimposed original current traces recorded at time points indicated by numerals.

Discussion

The present study demonstrates that the specific PI3K blocker LY294002 potently and reversibly inhibits the hKv1.5 current in a concentration-, time- and frequency-dependent manner. LY294002 has been widely used to examine the physiological and pathophysiological roles of PI3K in the regulation of various cellular functions (Knight *et al.*, 2004). However, the present experiments strongly suggested that the inhibitory

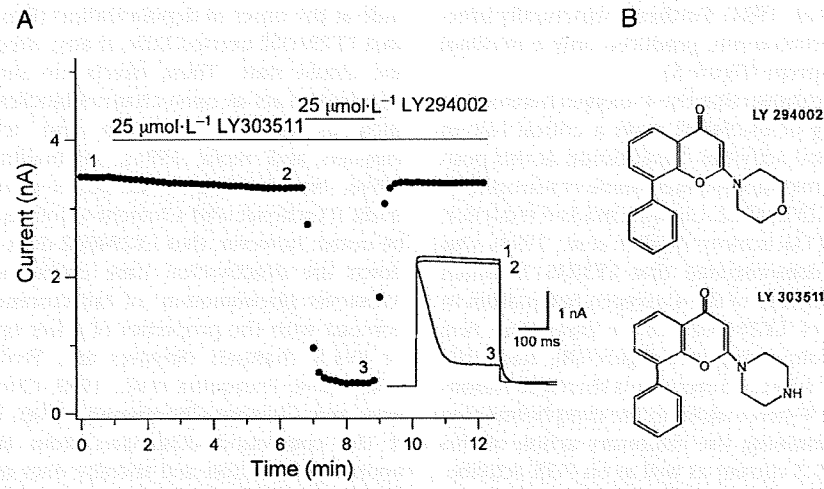

Figure 6 Effects of LY303511 on the human Kv1.5 current. (A) Human Kv1.5 current was activated by a protocol similar to that in Figure 5 in the presence of LY303511 and LY294002 (25 μmol·L^{-1}, each). (B) Chemical structures of LY294002 and LY303511. The morpholino oxygen in LY294002 is substituted by a nitrogen in LY303511, i.e., the morpholino ring becomes a piperazine ring.

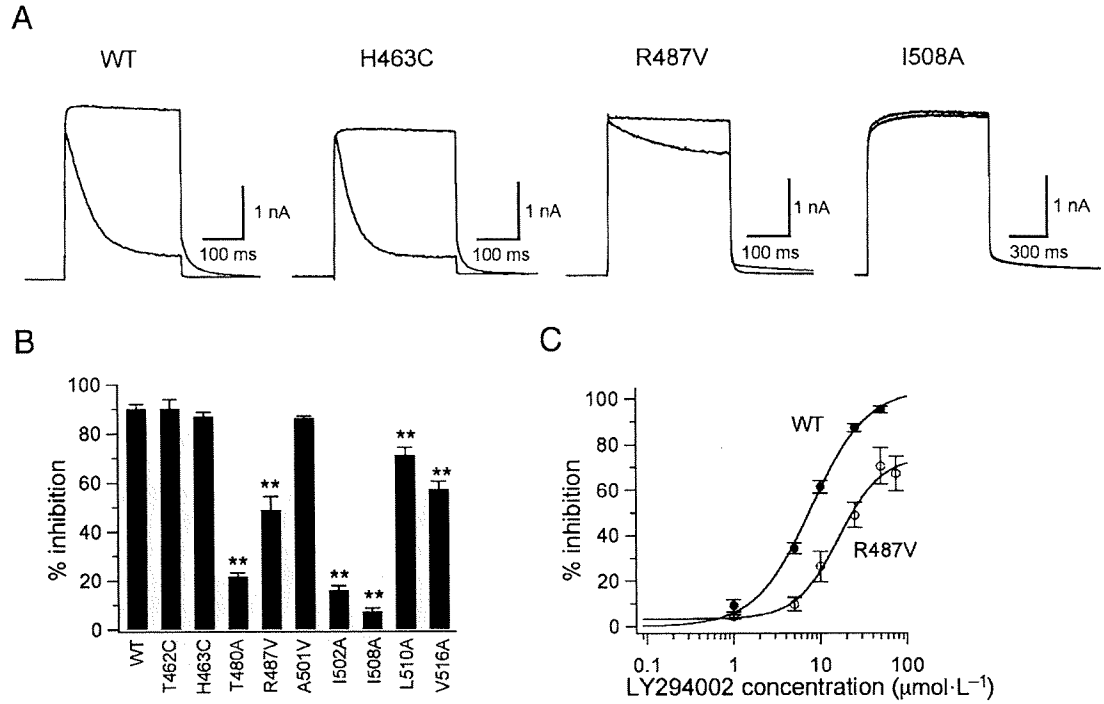

Figure 7 Inhibitory action of LY294002 on human Kv1.5 (hKv1.5) mutant channels. (A) Representative current traces recorded from wild-type (WT) and mutant channels (H463C and R487V) during 300 ms depolarizing step to +30 mV from a holding potential of −80 mV, followed by a 200 ms repolarization step to −40 mV before and during exposure to 25 μmol·L^{-1} LY294002. For I508A channels, because of slow kinetics, membrane potential was depolarized to +30 mV for 1 s, followed by a 1 s repolarization step to −40 mV. (B) Percentage inhibition of WT and various mutants of hKv1.5 channels by LY294002 (25 μmol·L^{-1}) was measured at the end of 300 ms depolarizing pulse. Numbers of cells are 6–16 in each channel. $^{**}P < 0.01$ compared with WT hKv1.5 channels. (C) Concentration – response relationship for LY294002 block of WT (●) and R487V (○) channels. The solid lines represent a least-squares fit of a Hill equation.

effect of LY294002 on hKv1.5 current was independent of PI3K signalling pathways for the following reasons. The block of hKv1.5 current takes place rapidly, within 10 s after addition of the compound, and reaches a steady-state inhibition within 1 min. This inhibitory effect was fully reversed in 1 min following removal of the compound (Figure 3). However, PI3K activity was completely abolished in 10 min by LY294002 (Vlahos *et al.*, 1994). Further, a structurally unrelated PI3K inhibitor, wortmannin, produced only a minimal effect on the hKv1.5 current (Figure 5).

Previous workers have shown that the 4′-oxygen heteroatom in the morpholine ring of LY294002 plays a critical role in determining its biological activities. Substitution at this position, with sulphur, hydroxymethyl, methylene or nitrogen, of the morpholine ring of LY294002, caused a marked reduction in the efficacy against PI3K activity (Vlahos *et al.*, 1994). Our present study clearly demonstrated that LY303511, which contains a 4′-nitrogen instead of the 4′-oxygen heteroatom in the morpholine ring of LY294002, i.e., a piperazine ring instead of the morpholine ring (see Figure 6B), had little inhibitory effect on the hKv1.5 current. It is therefore reasonable to assume that the 4′-heteroatom in the morpholine ring is also critical for determining the inhibitory action of this compound on the hKv1.5 current as well as on PI3K activity.

The action of LY294002 on the hKv1.5 currents can be best explained by block of the open channel, which is supported by the following experimental results. Firstly, LY294002 accelerated the hKv1.5 current decay during the depolarizing step in a concentration-dependent manner (Figure 2A,C). Next, LY294002 inhibition of hKv1.5 steeply increased at potentials between −30 and 0 mV, which corresponds to the voltage range of channel opening (Figure 1E). Then, LY294002 scarcely affected the activation time course of the channel and only modestly affected the peak amplitude at the onset of depolarization (Figs 1 and 2), suggesting that LY294002 exerted little, if any, effect on the channels in the closed state. These effects are similar to other drugs assumed to act as open-channel blockers of Kv1.5 channels, such as quinine, clofilium and tetrapentylammonium (Snyders and Yeola, 1995), zatebradine (Valenzuela *et al.*, 1996), bisindolylmaleimide (Choi *et al.*, 2000) and mibefradil (Perchenet and Clement-Chomienne, 2000). It should be noted, however, that LY294002 does not appreciably slow down the deactivation time course and fails to cause a 'crossover phenomenon' of tail current traces, which is in contrast with the properties of other open-channel blockers of Kv1.5 channels (Snyders and Yeola, 1995; Valenzuela *et al.*, 1996; Franqueza *et al.*, 1998; Choi *et al.*, 2000; Perchenet and Clement-Chomienne, 2000; Decher *et al.*, 2006). If the compound dissociates from the channel quickly upon repolarization and thereby does not interfere the time course for channel closure, nearly full amplitude of tail current (comparable to control conditions) is expected to appear. However, it is not the case for LY294002 (see

Figure 2A). Another possible explanation is that the functional dissociation of LY294002 from the channel that occurs upon repolarization may not interfere with the transition of the channel from an open to a closed state.

Previous studies have examined the molecular basis for high-affinity drug block of hKv1.5 channels (Yeola *et al.*, 1996; Decher *et al.*, 2004; 2006; Herrera *et al.*, 2005; Rezazadeh *et al.*, 2006). The anti-arrhythmic quinidine and the local anaesthetic benzocaine have been found to interact with Thr479 located near the pore helix and Thr507 and Val514 in the S6 domain of hKv1.5 channels (Snyders and Yeola, 1995; Yeola *et al.*, 1996; Caballero *et al.*, 2002). In recent years, Decher *et al.* (2004; 2006) and Eldstrom *et al.* (2007) have identified several amino acid residues (Thr479, Thr480, Val505, Ile508, Val512 and Val516) that could be essential for blocking action of S0100176 and AVE0118, using alanine scanning mutagenesis of the pore helix and S6 domain of the hKv1.5 channel. The present mutagenesis study has also found Thr480, Arg487, Ile502, Ile508, Leu510 and Val516 to be putative binding sites of LY294002. Of these six residues, Thr480, Ile508 and Val516 are believed to face towards the central cavity of the channel, whereas Ile502 and Leu510 are positioned away from the inner cavity (Decher *et al.*, 2004; Eldstrom *et al.*, 2007). It is therefore reasonable to propose that the reduced sensitivity of I502A and L510A mutants to LY294002 may be due to allosteric mechanisms, which alters the orientation of some amino acids towards the inner cavity of the channel.

A docking model has been used to compare the binding sites of novel atrial-selective, class III anti-arrhythmic compounds, such as S9947, MSD-D and ICAGEN-4 (Strutz-Seebohm *et al.*, 2007). This study suggests that hydrophobic interactions of the blocker molecules with Ile508 and Val512, as well as electrostatic interactions of the oxygen atoms of the inhibitor with the potassium ion in the selective filter Thr480 are important for the blocking action of these compounds. This binding complex formed by channel residues (selective filter), internal potassium ion and inhibitor oxygen was also proposed to be important for the binding of chromanol 293B to KCNQ1 (Kv7.1) channels (Lerche *et al.*, 2007). More recently, Andér *et al.* (2008) provided an improved model useful for further efforts to design ligands. These authors investigated binding of ortho,ortho-disubstituted bisaryl compounds to the open state of the hKv1.5 channels using a three-step procedure, including homology modelling, automated docking and binding free energy calculations, and suggested that, apart from the well-documented important residues Ile508, Val 512 and Val516 for ligand binding in the cavity, other residues, Ala509 and Pro513, also contribute to the non-polar binding interactions. Compared with the mutants I508A and T480A located deeper in the pore region, R487V at the outer mouth of the pore was found to partially attenuate LY294002 action (Figure 7 in the present study). We therefore propose that, as suggested for Ile502 and Leu510, an allosteric effect by the R487V mutation could be a possible explanation for the decreased potency of LY294002 on hKv1.5 channels.

Although the substitution of Arg (positively charged) by Val (neutral) at position 487 significantly reduced the inhibitory action of LY294002 (R487V, Figure 7B), we may exclude the possibility that this reduced sensitivity of the R487 mutant is related to some possible changes in electrostatic interaction between the residue and the compound, because the substitution of His (positively charged) by Cys (neutral) at position 463 (H463C) does not affect the sensitivity to LY294002 (Figure 7B). In addition, the substitution of neutral Ile by neutral Ala at positions 502 and 508 (I502A and I508A respectively) does markedly affect the LY294002 sensitivity. We also believe that the hydrophobicity and hydrophilicity of residues tested in the present study do not profoundly affect the sensitivity to inhibition by LY294002. For example, the replacement of His with Cys (hydropathy index changed from −3.2 to 2.5) at position 463 (Kyte and Doolittle, 1982) did not alter the sensitivity to LY294002, whereas the replacement of Arg with Val (hydropathy index changed from −4.5 to 4.2) at position 487 markedly reduced the sensitivity to LY294002 (Figure 7B).

Several hKv1.5 channel mutants (T480A, R487V and L510A) used for evaluating the blocking action have been shown to exhibit altered gating kinetics (Decher *et al.*, 2004; 2006; Rezazadeh *et al.*, 2006). However, there appears to be little, if any, clear evidence correlating the reduced sensitivity of these mutants to blockade, with possible kinetic changes. For example, T480A and V514A mutants exhibit similar slower changes in activation and deactivation rates (Decher *et al.*, 2005), but the responses to AVE0118 are very different between these two mutants (Decher *et al.*, 2006). In addition, the L510A mutant channel expressed in oocytes exhibits a pronounced inactivation, which is only slightly suppressed by AVE0118 (Decher *et al.*, 2006). In contrast, another novel channel blocker, S0100176, almost completely inhibits this mutant channel, as it does the WT channels (Decher *et al.*, 2004). These data suggest that the reduced affinity of LY294002 to hKv1.5 channel mutants is likely to be due to their changed binding sites, but probably not due to altered channel gating kinetics.

In the present study, we cannot completely rule out the possibility that inhibition of hKv1.5 current by LY294002 may be mediated, at least partly, through the inhibition of unidentified intracellular signalling pathways. However, an earlier study has confirmed that LY294002, which is a competitive inhibitor for the ATP binding site of PI3K, had no inhibitory effects on several other ATP-requiring, protein and lipid kinases, such as protein kinase A, protein kinase C, mitogen-activated protein (MAP) kinase, phosphatidylinositol 4-kinase and diacylglycerol kinase, when used at a concentration of 50 $\mu mol \cdot L^{-1}$ (Vlahos *et al.*, 1994). It is therefore reasonable to rule out the possible involvement of at least these ATP-requiring kinases in the inhibitory action of LY294002 on the hKv1.5 current.

LY303511 is an analogue of LY294002 that has no apparent effect on PI3K activity and thus provides a suitable control for evaluating cellular effects, unrelated to PI3K inhibition (Ding *et al.*, 1995). LY303511 has a marked inhibitory effect on cell proliferation and this effect is almost equal to that of LY294002 (Kristof *et al.*, 2005). It therefore seems likely that the substitution of an oxygen by nitrogen in LY303511 has little effects on its membrane permeability. In additional experiments, we have confirmed that the hKv1.5 current is not appreciably decreased, even by prolonging the exposure

time to 25 μmol·L^{-1} LY303511 to more than 10 min (data not shown). The present study clearly demonstrates that LY303511 has little effect on hKv1.5 current (Figure 6), which provides some structural basis to the suggestion that the morpholino oxygen is crucially involved in producing the inhibitory action of LY294002 on hKv1.5 currents. It is interesting to note that endogeneous Kv channels in MIN6 insulinoma cells and Kv2.1 channels heterologously expressed in tsA201 cells are substantially inhibited not only by LY294002, but also by LY303511 (El-Kholy *et al.*, 2003). Such a difference in the effect of LY303511 on hKv1.5 and other Kv channels may also support some specific functional role of the morpholino oxygen for the inhibition of hKv1.5 channels. The present study may thus provide some important hints for future development of effective and specific blockers for hKv1.5 channels.

Acknowledgements

The authors would like to thank Dr D Fedida for kindly providing the mammalian expression vector pcDNA3.1 containing hKv1.5 cDNA. This study was supported by Grant-in-Aid for Scientific Research (Nos. 17590185 to H.M. and 19390212 to M.H.) from Japan Society for the Promotion of Science, and by grants from the National Basic Research Program of China (973 Program, No. 2007CB512005 to WJZ).

Conflicts of interest

None.

References

Alexander SP, Mathie A, Peters JA (2008). Guide to Receptors and Channels (GRAC), 3rd edition. *Br J Pharmacol* **153** (Suppl 2): S1–S209.

Andér M, Luzhkov VB, Åqvist J (2008). Ligand binding to the voltage-gated Kv1.5 potassium channel in the open state – docking and computer simulations of a homology model. *Biophys J* **94**: 820–831.

Brendel J, Peukert S (2003). Blockers of the Kv1.5 channel for the treatment of atrial arrhythmias. *Curr Med Chem Cardiovasc Hematol Agents* **1**: 273–287.

Bril A (2002). Recent advances in arrhythmia therapy: treatment and prevention of atrial fibrillation. *Curr Opin Pharmacol* **2**: 154–159.

Caballero R, Moreno I, Gonzalez T, Valenzuela C, Tamargo J, Delpon E (2002). Putative binding sites for benzocaine on a human cardiac cloned channel (Kv1.5). *Cardiovasc Res* **56**: 104–117.

Choe H, Lee YK, Lee YT, Choe H, Ko SH, Joo CU *et al.* (2003). Papaverine blocks hKv1.5 channel current and human atrial ultrarapid delayed rectifier K$^+$ currents. *J Pharmacol Exp Ther* **304**: 706–712.

Choi BH, Choi JS, Jeong SW, Hahn SJ, Yoon SH, Jo YH *et al.* (2000). Direct block by bisindolylmaleimide of rat Kv1.5 expressed in Chinese hamster ovary cells. *J Pharmacol Exp Ther* **293**: 634–640.

Chugh SS, Blackshear JL, Shen WK, Hammill SC, Gersh BJ (2001). Epidemiology and natural history of atrial fibrillation: clinical implications. *J Am Coll Cardiol* **37**: 371–378.

Crijns HJ, Van Gelder IC, Walfridsson H, Kulakowski P, Ronaszeki A, Dedek V *et al.* (2006). Safe and effective conversion of persistent atrial fibrillation to sinus rhythm by intravenous AZD7009. *Heart Rhythm* **3**: 1321–1331.

Decher N, Pirard B, Bundis F, Peukert S, Baringhaus KH, Busch AE *et al.* (2004). Molecular basis for Kv1.5 channel block: conservation of drug binding sites among voltage-gated K$^+$ channels. *J Biol Chem* **279**: 394–400.

Decher N, Kumar P, Gonzalez T, Renigunta V, Sanguinetti MC (2005). Structural basis for competition between drug binding and Kvβ 1.3 accessory subunit-induced N-type inactivation of Kv1.5 channels *Mol Pharmacol* **68**: 995–1005.

Decher N, Kumar P, Gonzalez T, Pirard B, Sanguinetti MC (2006). Binding site of a novel Kv1.5 blocker: a 'foot in the door' against atrial fibrillation. *Mol Pharmacol* **70**: 1204–1211.

Ding J, Vlahos CJ, Liu R, Brown RF, Badwey JA (1995). Antagonists of phosphatidylinositol 3-kinase block activation of several novel protein kinases in neutrophils. *J Biol Chem* **270**: 11684–11691.

Dorian P, Pinter A, Mangat I, Korley V, Cvitkovic SS, Beatch GN (2007). The effect of vernakalant (RSD1235), an investigational antiarrhythmic agent, on atrial electrophysiology in humans. *J Cardiovasc Pharmacol* **50**: 35–40.

Eldstrom J, Choi WS, Steek DF, Fedida D (2003). SAP97 increases Kv1.5 currents through an indirect N-terminal mechanism. *FEBS lett* **547**: 205–211.

Eldstrom J, Wang Z, Xu H, Pourrier M, Ezrin A, Gibson K *et al.* (2007). The molecular basis of high-affinity binding of the antiarrhythmic compound vernakalant (RSD1235) to Kv1.5 channels. *Mol Pharmacol* **72**: 1522–1534.

El-Kholy W, Macdonald PE, Lin JH, Wang J, Fox JM, Light PE *et al.* (2003). The phosphatidylinositol 3-kinase inhibitor LY294002 potently blocks K(V) currents via a direct mechanism. *FASEB J* **17**: 720–732.

Fedida D, Wible B, Wang Z, Fermini B, Faust F, Nattel S *et al.* (1993). Identity of a novel delayed rectifier current from human heart with a cloned K$^+$ channel current. *Circ Res* **73**: 210–216.

Feng J, Xu D, Wang Z, Nattel S (1998). Ultrarapid delayed rectifier current inactivation in human atrial myocytes: properties and consequences. *Am J Physiol* **275**: H1717–H1725.

Franqueza L, Valenzuela C, Delpón E, Longobardo M, Caballero R, Tamargo J (1998). Effects of propafenone and 5-hydroxypropafenone on hKv1.5 channels. *Br J Pharmacol* **125**: 969–978.

Gamper N, Fillon S, Huber SM, Feng Y, Kobayashi T, Cohen P *et al.* (2002). IGF-1 upregulates K$^+$ channels via PI3-kinase, PDK1 and SGK1. *Pflugers Arch* **443**: 625–634.

Hamill OP, Marty A, Neher E, Sakmann B, Sigworth FJ (1981). Improved patch-clamp techniques for high-resolution current recording from cells and cell-free membrane patches. *Pflugers Arch* **391**: 85–100.

Herrera D, Mamarbachi A, Simoes M, Parent L, Sauve R, Wang Z *et al.* (2005). A single residue in the S6 transmembrane domain governs the differential flecainide sensitivity of voltage-gated potassium channels. *Mol Pharmacol* **68**: 305–316.

Knight ZA, Chiang GG, Alaimo PJ, Kenski DM, Ho CB, Coan K *et al.* (2004). Isoform-specific phosphoinositide 3-kinase inhibitors from an arylmorpholine scaffold. *Bioorg Med Chem* **12**: 4749–4759.

Knobloch K, Brendel J, Peukert S, Rosenstein B, Busch AE, Wirth KJ (2002). Electrophysiological and antiarrhythmic effects of the novel I(Kur) channel blockers, S9947 and S20951, on left vs. right pig atrium in vivo in comparison with the I(Kr) blockers dofetilide, azimilide, d,l-sotalol and ibutilide. *Naunyn Schmiedebergs Arch Pharmacol* **366**: 482–487.

Knobloch K, Brendel J, Rosenstein B, Bleich M, Busch AE, Wirth KJ (2004). Atrial-selective antiarrhythmic actions of novel Ikur vs. Ikr, Iks, and IKAch class Ic drugs and beta blockers in pigs. *Med Sci Monit* **10**: BR221–228.

Kristof AS, Pacheco-Rodriguez G, Schremmer B, Moss J (2005). LY303511 (2-Piperazinyl-8- phenyl-4*H*-1-benzopyran-4-one) Acts via Phosphatidylinositol 3-Kinase-Independent Pathways to Inhibit Cell Proliferation via Mammalian Target of Rapamycin (mTOR)-

and Non-mTOR-Dependent Mechanisms. *J Pharmacol Exp Ther* **314**: 1134–1143.

Kyte J, Doolittle RF (1982). A simple method for displaying the hydropathic character of a protein. *J Mol Biol* **157**: 105–132.

Lerche C, Bruhova I, Lerche H, Steinmeyer K, Wei AD, Strutz-Seebohm N *et al.* (2007). Chromanol 293B binding in KCNQ1 (Kv7.1) channels involves electrostatic interactions with a potassium ion in the selectivity filter. *Mol Pharmacol* **71**: 1503–1511.

Li GR, Feng J, Yue L, Carrier M, Nattel S (1996). Evidence for two components of delayed rectifier K^+ current in human ventricular myocytes. *Circ Res* **78**: 689–696.

Nattel S, Yue L, Wang Z (1999). Cardiac ultrarapid delayed rectifiers: a novel potassium current family o f functional similarity and molecular diversity. *Cell Physiol Biochem* **9**: 217–226.

Perchenet L, Clement-Chomienne O (2000). Characterization of mibefradil block of the human heart delayed rectifier hKv1.5. *J Pharmacol Exp Ther* **295**: 771–778.

Powis G, Bonjouklian R, Berggren MM, Gallegos A, Abraham R, Ashendel C *et al.* (1994). Wortmannin, a potent and selective inhibitor of phosphatidylinositol-3-kinase. *Cancer Res* **54**: 2419–2423.

Regan CP, Stump GL, Wallace AA, Anderson KD, McIntyre CJ, Liverton NJ *et al.* (2007). In vivo cardiac electrophysiologic and antiarrhythmic effects of an isoquinoline IKur blocker, ISQ-1, in rat, dog, and nonhuman primate. *J Cardiovasc Pharmacol* **49**: 236–245.

Rezazadeh S, Claydon TW, Fedida D (2006). KN-93 (2-[N-(2-hydroxyethyl)]-N-(4-methoxybenzenesulfonyl)]amino-N-(4-chlorocinnamyl)-N-methylbenzylamine), a calcium/calmodulin-dependent protein kinase II inhibitor, is a direct extracellular blocker of voltage-gated potassium channels. *J Pharmacol Exp Ther* **317**: 292–299.

Snyders DJ, Tamkun MM, Bennett PB (1993). Arapidly activating and slowly inactivating potassium channel cloned from human heart. Functional analysis after stable mammalian cell culture expression. *J Gen Physiol* **101**: 513–543.

Snyders DJ, Yeola SW (1995). Determinants of antiarrhythmic drug action. Electrostatic and hydrophobic components of block of the human cardiac hKv1.5 channel. *Circ Res* **77**: 575–583.

Strutz-Seebohm N, Gutcher I, Decher N, Steinmeye K, Lang F, Seebohm G (2007). Comparison of potent Kv1.5 potassium channel inhibitors reveals the molecular basis for blocking kinetics and binding mode. *Cell Physiol Biochem* **20**: 791–800.

Trotter BW, Nanda KK, Kett NR, Regan CP, Lynch JJ, Stump GL (2006). Design and synthesis of novel soquinoline-3-nitriles as orally bioavailable Kv1.5 antagonists for the treatment of atrial fibrillation. *J Med Chem* **49**: 6954–6957.

Valenzuela C, Delpón E, Franqueza L, Gay P, Pérez O, Tamargo J *et al.* (1996). Class III antiarrhythmic effects of zatebradine. Time-, state-, use-, and voltage-dependent block of hKv1.5 channels. *Circulation* **94**: 562–570.

Varro A, Biliczki P, Iost N, Virag L, Hala O, Kovacs P *et al.* (2004). Theoretical possibilities for the development of novel antiarrhythmic drugs. *Curr Med Chem* **11**: 1–11.

Vlahos CJ, Matter WF, Hui KY, Brown RF (1994). A specific inhibitor of phosphatidylinositol 3-kinase, 2-(4-morpholinyl)-8-phenyl-4H-1-benzopyran-4-one (LY294002). *J Biol Chem* **269**: 5241–5248.

Vos MA (2004). Atrial-specific drugs: the way to treat atrial fibrillation? *J Cardiovasc Electrophysiol* **15**: 1451–1452.

Wang Z, Fermini B, Nattel S (1993). Sustained depolarization-induced outward current in human atrial myocytes: evidence for a novel delayed rectifier K^+ current similar to Kv1.5 cloned channel currents. *Circ Res* **73**: 1061–1076.

Wettwer E, Hala O, Christ T, Heubach JF, Dobrev D, Knaut M *et al.* (2004). Role of Ikur in controlling action potential shape and contractility in the human atrium. Influence of chronic atrial fibrillation. *Circulation* **110**: 2299–2306.

Yeola SW, Rich TC, Uebele VN, Tamkun MM, Snyders DJ (1996). Molecular analysis of a binding site for quinidine in a human cardiac delayed rectifier K^+ channel. Role of S6 in antiarrhythmic drug binding. *Circ Res* **78**: 1105–1114.

Acknowledgements

We thank Ms. Kirsten Skarratt, who performed the genotyping, and the Nepean Hospital staff with assistance in recruiting subjects.

References

[1] McLean AS, Eslick GD, Coats AJS. The epidemiology of heart failure in Australia. Int J Cardiol 2007;118:370–4.
[2] Naito Y, Tsujino T, Fujioka Y, Ohyanagi M, Okamura H, Iwasaki T. Increased circulating interleukin-18 in patients with congestive heart failure. Heart 2002;88:296–7.
[3] Yamaoka-Tojo M, Taiki T, Takauki I, Yoji M, Kazuyuki O, Tohru I. Circulating levels of Interleukin 18 reflect etiologies of heart failure: Th1/Th2 cytokine imbalance exaggerates the pathophysiology of advanced heart failure. J Card Fail 2002;8:21–7.
[4] Mallat Z, Heymes C, Corbaz A, et al. Evidence for altered interleukin 18 (IL)-18 pathway in human heart failure. FASEB J 2004;18:1752–4.
[5] Sluyter R, Dalitz JG, Wiley JS. P2X7 receptor polymorphism impairs extracellular adenosine 5′-triphosphate-induced interleukin-18 release from human monocytes. Genes Immun 2004;5:588–91.
[6] Shemon AN, Sluyter R, Fernando SL, et al. A Thr357 to Ser polymorphism in homozygous and compound heterozygous subjects causes absent or reduced P2X7 function and impairs ATP-induced mycobacterial killing by macrophages. J Biol Chem 2006;281:2079–86.

0167-5273/$ - see front matter
doi:10.1016/j.ijcard.2008.05.017

A novel *KCNH2* mutation as a modifier for short QT interval

Hideki Itoh [a], Tomoko Sakaguchi [a], Takashi Ashihara [a], Wei-Guang Ding [b], Iori Nagaoka [a], Yuko Oka [a], Yuko Nakazawa [a], Takenori Yao [a], Hikari Jo [a], Makoto Ito [a], Kazufumi Nakamura [c], Tohru Ohe [c], Hiroshi Matsuura [b], Minoru Horie [a,*]

[a] *Department of Cardiovascular and Respiratory Medicine, Shiga University of Medical Science, Seta Tsukinowa-cho, Otsu, Shiga, 520-2192, Japan*
[b] *Department of Physiology, Shiga University of Medical Science, Seta Tsukinowa-cho, Otsu, Shiga, 520-2192, Japan*
[c] *Department of Cardiovascular Medicine, Okayama University Graduate School of Medicine, Dentistry and Pharmaceutical Sciences, Okayama, 700-8558, Japan*

Received 24 January 2008; Accepted 3 May 2008
Available online 9 August 2008

Abstract

In a 34-year-old man showing short QT interval (QTc 329 ms), we identified a novel C-terminal *KCNH2* mutation, R1135H. Using a heterologous expression system with CHO cells, the mutant channels were found to display a significantly slow deactivation, which resulted in a gain-of-function for reconstituted 'I_{Kr}' channels. This mutation could modify clinical phenotypes for this patient.

Keywords: Short QT syndrome; Brugada syndrome; *KCNH2*; Mutation; Sudden death

Recently, the short QT interval has been shown to be associated with ventricular tachycardia or familial sudden cardiac death [1]. In 2004, Brugada et al. reported the first mutation associated with the short QT syndrome [2], and since then several disease-causing genes for the short QT syndrome have been identified [2–4]. In this letter, we describe a novel C-terminal *KCNH2* mutation, R1135H, in a proband with short QT interval. Expression of the mutant channels on CHO cells did not display the altered inactivation seen by N588K in the *KCNH2*, but slowed down the deactivation process significantly, which resulted in the "gain-of-function" of I_{Kr} and shortened the QT interval.

A 34-year-old man was admitted to the hospital because of analyses for the ECG abnormality. His electrocardiogram

* Corresponding author. Department of Cardiovascular and Respiratory Medicine, Shiga University of Medical Science, Seta Tsukinowa-cho, Otsu, Shiga, 520-2192, Japan. Fax: +81 77 543 5839.
E-mail address: horie@belle.shiga-med.ac.jp (M. Horie).

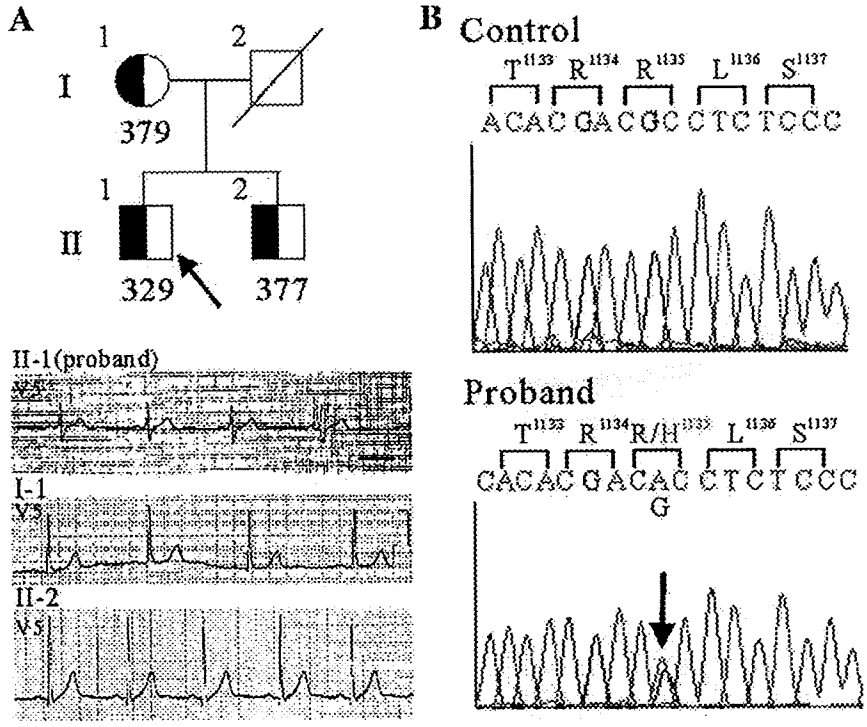

Fig. 1. Clinical and molecular genetic observations. A, Partial pedigree of the family (circles indicate females, squares males) and ECGs. The half-filled symbol represents the mutation carriers, A arrow, the proband. QTc intervals are shown below each symbol. B, Part of the nucleotide sequence of the *KCNH2* exon 15 showing G-to-A transition (arrow). The mutation changes the Arg codon (AAC) in wild-type to His (AGC).

(II-1, Fig. 1A) showed marked QT shortening (QTc 329 ms) as well as Brugada-type ECG. Both PQ interval and QRS width were within normal range, and the QT interval normalized except in bradycardia. Holter monitoring test revealed the presence of non-sustained ventricular tachycardia in night. Underlying structural heart diseases were excluded by ultrasound cardiography and magnetic resonance imaging. In the subsequent electrophysiological study, ventricular fibrillation was easily and repeatedly inducible by triple premature stimulation to the right ventricular outflow tract, and the index patient received an implantable cardioverter defibrillator. His 30-year-old brother (II-2, Fig. 1A) had a non-documented arrhythmia, but his ECG showed relatively shortened QT interval (QTc 377 ms). His mother (II-1, Fig. 1A) remained asymptomatic but her ECGs showed bradycardia with slightly shortened QT interval (QTc 379 ms).

PCR-DHPLC analyses revealed an aberrant peak band in exon 15 of *KCNH2* in the proband. The pattern was not observed in controls consisting of 200 chromosomes, suggesting that this abnormality represents a disease-related mutation. DNA sequencing confirmed a G-to-A transition leading to amino acid substitution of histidine for arginine at codon 1135 (R1135H) (Fig. 1B), located in the end of the C-terminal region of *KCNH2*. The proband had no mutations for other genes known responsible for short QT and Brugada syndromes, including *SCN5A* and *CACNA1C* [5]. Genetic analyses for proband's mother and younger brother revealed that they had the same heterozygous R1135H.

The R1135H mutant expressed functional channels in CHO cells with apparently slowed and larger tail currents (Fig. 2A and B). The other properties and kinetics of mutant channels were not altered compared to those of the wild type, including activation and inactivation gates. To date, there is only a single report of gain-of-function *KCNH2* mutation responsible for the short QT syndrome, N588K [2]. Brugada et al. identified this mutation in the S5-P loop region of I_{Kr} channel in two unrelated families with hereditary short QT syndrome. Functional analyses of N588K channels showed that it caused a complete loss of rectifying properties of I_{Kr} channels and did not inactivate over the physiological range of potentials. Therefore the mechanism for a gain-of-function of R1135H appeared quite different from that of N588K and unique in inducing the short QT syndrome.

It remains unknown why the proband alone showed a Brugada ECG pattern. *SCN5A* mutations have been reported in ~20% of patients with Brugada syndrome [6]. Brugada syndrome has wide genetic heterogeneity, and other genes are thought to be involved in the generation of the syndrome. In our index patient, some unknown genetic variant, for example *CACNB2* encoding cardiac calcium channel β2 subunit [5], might be inherited from his paternal side, in

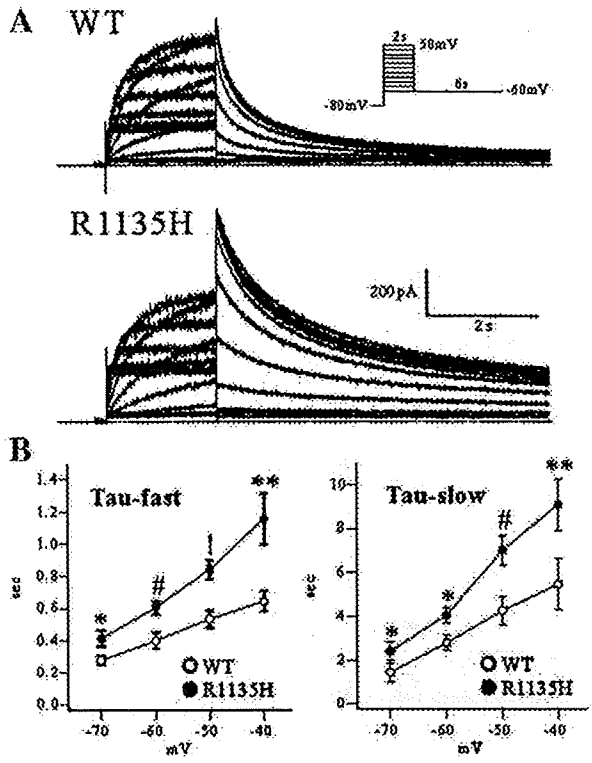

Fig. 2. Analysis of whole-cell current recorded from CHO cells expressing WT or R1135H. A, Traces of I_{Kr} for WT and R1135H channels. The inset illustrates the voltage protocol. B, Time course of deactivation for WT and R1135H channels. To examine the deactivation time course, a conditioning pulse to +40 mV from a holding potential of −80 mV was followed by hyperpolarizing test pulses between −70 mV and −40 mV for 16 s. Deactivation time constants were measured by fitting deactivating currents during test pulses at each potential with double exponentials. Both components of Tau for mutants were larger than that of WT; $*p<0.05$, $**p<0.01$, $\#p<0.001$, $!p<0.005$.

which there were 2 cases of sudden death during sleep and play a role in expressing the phenotype of Brugada syndrome.

0167-5273/$ - see front matter © 2008 Elsevier Ireland Ltd. All rights reserved.
doi:10.1016/j.ijcard.2008.05.050

Acknowledgements

This work was supported by the Grant-in-Aid for Young Scientists (H.I.) and the Grant-in-Aid for Scientific Research (M.H.).

References

[1] Gussak I, Brugada P, Brugada J, et al. Idiopathic short QT interval: a new clinical syndrome? Cardiology 2000;94:99–102.
[2] Brugada R, Hong K, Dumaine R, et al. Sudden death associated with short-QT syndrome linked to mutations in HERG. Circulation 2004;109:30–5.
[3] Bellocq C, van Ginneken AC, Bezzina CR, et al. Mutation in the KCNQ1 gene leading to the short QT-interval syndrome. Circulation 2004;109:237–2394.
[4] Priori SG, Pandit SV, Rivolta I, et al. A novel form of short QT syndrome (SQT3) is caused by a mutation in the KCNJ2 gene. Circ Res 2005;96:800–7.
[5] Antzelevitch C, Pollevick GD, Cordeiro JM, et al. Loss-of-function mutations in the cardiac calcium underlie a new clinical entity characterized by ST-segment elevation, short QT intervals, and sudden cardiac death. Circulation 2007;115:442–9.
[6] Priori SG, Napolitano C, Gasparini M, et al. Clinical and genetic heterogeneity of right bundle branch block and ST-segment elevation syndrome: a prospective evaluation of 52 families. Circulation 2000;102:2509–15.

Cholesteryl Ester Transfer Protein, Coronary Calcium, and Intima-Media Thickness of the Carotid Artery in Middle-Age Japanese Men

Tomonori Okamura, MD[a,b,*], Akira Sekikawa, MD[c], Takashi Kadowaki, MD[b], Aiman El-Saed, MD[c], Robert D. Abbott, PhD[d], J. David Curb, MD[e], Daniel Edmundowicz, MD[c], Yasuyuki Nakamura, MD[f], Kiyoshi Murata, MD[b], Atsunori Kashiwagi, MD[b], Kim Sutton-Tyrrell, DrPH[c], Rhobert W. Evans, PhD[c], Joseph M. Zmuda, PhD[c], Hiroshi Maegawa, MD[b], Atsushi Hozawa, MD[b], Ken-Ichi Mitsunami, MD[b], Yoshihiko Nishio, PhD[b], Iva Miljkovic-Gacic, MD[c], Minoru Horie, MD[b], Naomi Miyamatsu, MD[b], Yoshitaka Murakami, PhD[b], Lewis H. Kuller, MD[c], and Hirotsugu Ueshima, MD[b]

The relation between cholesteryl ester transfer protein (CETP) levels and atherosclerosis is controversial. We examined whether the serum CETP levels were associated with subclinical atherosclerosis, independent of its most common gene variant, in a sample of Japanese men. A population-based cross-sectional study of 250 Japanese men aged 40 to 49 years was conducted to assess the intima-media thickness of the carotid artery, coronary artery calcium, serum CETP levels, and the CETP D442G gene variant. Compared with the lowest CETP quartile, the multivariate adjusted odds ratio for coronary artery calcium was 0.77 (95% confidence interval 0.18 to 3.36), 0.96 (95% confidence interval 0.27 to 3.40), and 3.49 (95% confidence interval 1.05 to 11.6) with increasing CETP quartiles. The serum CETP quartiles were also positively associated with the intima-media thickness of the carotid artery (adjusted mean 602, 616, 615, and 646 μm for the lowest to top quartile, respectively). The findings remained unchanged after additional adjustment for the CETP D442G gene variant. No significant difference was found in the prevalence of coronary artery calcium or in the mean intima-media thickness of the carotid artery between participants with and without the CETP D442G gene variant. **(Am J Cardiol 2009;104:818–822)**

The cholesteryl ester transfer protein (CETP) plays a major role in exchanging cholesteryl esters in high-density lipoprotein (HDL) particles and triglycerides (TG) in apolipoprotein B-containing lipoproteins.[1] The purpose of the present study was to examine the relation between the serum CETP levels and subclinical atherosclerosis, such as coronary calcium and the carotid intima-media thickness (IMT), in a Japanese population with much lower prevalence of coronary heart disease (CHD) than that of Western populations.[2,3] Our a priori hypothesis was that the serum CETP levels would be positively associated with subclinical atherosclerosis, irrespective of the CETP D442G missense mutation, which is common in the Japanese.[4] Therefore, we performed a cross-sectional study of Japanese men in a narrow age range who were randomly selected from a surveyed community.

Methods

The participants of the present study were Japanese men from a cross-sectional study comparing subclinical atherosclerosis findings between the United States and Japan.[5–8] A total of 313 Japanese men aged 40 to 49 years (from Kusatsu City, Shiga, Japan) were randomly selected from resident registration of the city office. The exclusion criteria were (1) clinical cardiovascular disease, (2) type 1 diabetes, (3) cancer, except for previous skin cancer, (4) renal failure, (5) genetic familial hyperlipidemia. Of the 313 participants, 63 were excluded for the following reasons: informed consent for genetic analysis outside of Japan was not obtained (n = 14), genotype failure because of technical problems or a lack of blood samples (n = 46), and missing information (n = 3). Thus, we analyzed the data from 250 participants, all of whom provided informed consent. The institutional review boards of Shiga University of Medical Science and the University of Pittsburgh approved the present study.

[a]Preventive Cardiology, National Cardiovascular Center, Suita, Osaka, Japan; [b]Shiga University of Medical Science, Otsu, Shiga, Japan; [c]University of Pittsburgh, Pittsburgh, Pennsylvania; [d]University of Virginia, Charlottesville, Virginia; [e]University of Hawaii, Honolulu, Hawaii; [f]Kyoto Women's University, Kyoto, Kyoto, Japan. Manuscript received March 31, 2009; revised manuscript received and accepted May 2, 2009.

This research was supported by Grants R01 HL68200 and HL071561 from the National Institutes of Health, Bethesda, Maryland; by a Grant-in-Aid for Scientific Research, Grants C18590595 and C20590670, from the Japan Society for the Promotion of Science, Tokyo, Japan; and by a Grant-in-Aid for Scientific Research, Grant A13307016, by the Japanese Ministry of Education, Culture, Sports, Science and Technology, Tokyo, Japan.

*Corresponding author: Tel: (+81) 6-6833-5012, ext. 2228 or 2188; fax: (+81) 6-6833-5300.

E-mail address: okamurat@hsp.ncvc.go.jp (T. Okamura).

0002-9149/09/$ – see front matter
doi:10.1016/j.amjcard.2009.05.021

Table 1
Risk characteristics stratified by cholesteryl ester transfer protein quartile in 250 Japanese men aged 40 to 49 years, Kusatsu City, Shiga, Japan, 2002–2004

Cardiovascular Risk Factors	CETP Quartile (mg/L)				p for Trend
	Q1 (≤1.9; n = 56)	Q2 (2.0–2.1; n = 56)	Q3 (2.2–2.5; n = 73)	Q4 (≥2.6; n = 65)	
CETP (stratum mean) (mg/L)	1.72 ± 0.20	2.05 ± 0.05	2.31 ± 0.11	2.86 ± 0.29	
Age (years)	45.1 ± 2.6	44.3 ± 2.6	45.8 ± 2.7	45.0 ± 2.8	0.47
Body mass index (kg/m^2)	23.5 ± 3.1	23.6 ± 3.5	24.4 ± 2.9	23.7 ± 3.1	0.49
Waist (cm)	84.8 ± 8.1	84.7 ± 9.4	87.1 ± 7.4	84.8 ± 8.8	0.27
LDL cholesterol (mmol/L)	2.96 ± 0.68	2.96 ± 0.85	3.72 ± 0.82	3.71 ± 0.96	<0.01
HDL cholesterol (mmol/L)	1.50 ± 0.40	1.42 ± 0.36	1.31 ± 0.28	1.37 ± 0.30	<0.01
Triglycerides* (mmol/L)	1.49	1.58	1.61	1.63	0.27
Hypertension	18 (32%)	18 (32%)	22 (30%)	13 (20%)	0.14
Diabetes	4 (7.1%)	2 (3.6%)	4 (5.5%)	5 (7.7%)	0.78
Metabolic syndrome	12 (21%)	12 (21%)	20 (27%)	14 (22%)	0.80
Current smoker	34 (61%)	31 (55%)	35 (48%)	28 (43%)	0.04
Current alcohol drinker	46 (82%)	44 (79%)	45 (62%)	34 (52%)	<0.01
Lipid-lowering medication use	1 (1.8%)	3 (5.4%)	4 (5.5%)	1 (1.5%)	0.93
CETP D442G mutation	11 (20%)	1 (1.8%)	0 (0%)	2 (3.1%)	0.01
Intima-media thickness (μm)					
Common carotid artery	602 ± 77	611 ± 67	624 ± 85	640 ± 81	0.05
Average (μm)	605 ± 78	603 ± 54	622 ± 77	635 ± 71	0.21
Plaque in carotid artery	2 (3.6%)	0 (0%)	4 (5.5%)	6 (9.2%)	0.06
Coronary artery calcium	5 (8.9%)	4 (7.1%)	8 (11.0%)	14 (21.5%)	0.03

Data are presented as mean ± SD for continuous variables or numbers (%) for categorical variables.
* Geometric mean.
CETP = cholesteryl ester transfer protein; HDL = high-density lipoprotein; LDL = low-density lipoprotein; Q = quartile.

The samples for CETP measurement were shipped on dry ice to 1 laboratory in Japan (SRL, Tokyo, Japan). Serum CETP were measured by an enzyme-linked immunosorbent assay with 2 different monoclonal antibodies.[9] The interassay coefficient of variation was 4.41% and the intra-assay coefficient of variation was 2.57%. Other samples were shipped to the Heinz Laboratory at the University of Pittsburgh (Pittsburgh, Pennsylvania), where the serum total cholesterol, low-density-lipoprotein cholesterol, HDL cholesterol, TG, and glucose were measured. Diabetes was defined as a fasting blood glucose level of ≥7.0 mmol/L (≥126 mg/dl) or the use of diabetic medications, or both.

Blood pressure was measured using an automated sphygmomanometer (BP-8800, Colin Medical Technology, Komaki, Japan). Hypertension was defined as systolic blood pressure ≥140 mm Hg, diastolic blood pressure ≥90 mm Hg, the use of antihypertensive medications, or any combination of these. The body mass index was calculated as the weight in kilograms divided by the square of the height in meters. The waist circumference was measured at the umbilical level. The metabolic syndrome was defined according to the modified National Cholesterol Education Program-Adult Treatment Panel III criteria.[10] Current smoking and drinking were assessed by a self-administered questionnaire. Current drinkers were defined as those who consumed alcohol ≥2 times/wk.

Genotyping was completed using genomic DNA prepared from buffy coats. The CETP D442G missense mutation (rs2303790) was genotyped using the fluorogenic 5′-nuclease TaqMan allelic discrimination assay (Applied Biosystems, Foster City, California). The assays were performed under standard conditions on a 7900HT real-time polymerase chain reaction instrument, with probes and reagents purchased from Applied Biosystems (Foster City, California). The allele and genotype counts were in Hardy-Weinberg equilibrium.

Heart scanning was performed using a GE-Imatron C150 EBCT scanner (GE Medical Systems, South San Francisco, California) to obtain 30 to 40 contiguous 3-mm-thick transverse images from the level of the aortic root to the apex of the heart. The images were obtained during a maximal breath hold using electrocardiographic triggering (60% of RR interval) so that each 100 ms exposure was obtained during the same phase of the cardiac cycle. One trained reader at the Cardiovascular Institute, University of Pittsburgh, read the images, using a Digital Imaging and Communications in Medicine workstation and software from AccuImage (AccuImage Diagnostic, San Francisco, California). The software program implements the widely accepted Agatston scoring method.[11] The reproducibility of the EBCT scans had an intraclass correlation of 0.98.[5–8] In the present study, coronary artery calcium (CAC) was defined as absent for a coronary calcium score of <10 and present for a coronary calcium score of ≥10.

The carotid scanning procedures have been previously described.[5,8] Before the study began, sonographers received a 3-day training session for carotid scanning provided by the Ultrasound Research Laboratory, University of Pittsburgh. We also applied continuous quality assessment programs developed by the laboratory to ensure the scanning quality.[12] Using these programs, the certified sonographers scanned and the certified reader read the scanned images. A Toshiba 140A scanner equipped with a 7.5-MHz linear array imaging probe was used. The sonographers scanned the right and left common carotid arteries, carotid bulbs, and internal carotid arteries. The trained readers digitized the

Table 2
Age and multivariate-adjusted ORs (95% CIs) for coronary calcification (coronary calcium score ≥10) comparing top 3 quartiles and bottom quartile of serum cholesteryl ester transfer protein (CETP) in 250 Japanese men aged 40 to 49 years, Kusatsu City, Shiga, Japan, 2002–2004

Variable	Q1 (≤1.9; Referent)	Q2 (2.0–2.1)		Q3 (2.2–2.5)		Q4 (>2.6)		1-mg/L Increase
		OR	95% CI	OR	95% CI	OR	95% CI	
Japanese men (n)	56	56		73		65		
Age-adjusted	1.00	0.90	0.23–3.60	1.09	0.33–3.61	2.89	0.96–8.75	2.57 (1.14–5.79)
Multivariate adjusted								
Model 1*	1.00	0.77	0.18–3.36	0.96	0.27–3.40	3.49	1.05–11.6	3.07 (1.22–7.72)
Model 2†	1.00	0.79	0.18–3.57	1.01	0.26–3.87	3.64	1.03–12.9	3.26 (1.28–8.34)

* Adjusted for age, body mass index, hypertension, diabetes, triglycerides (log-transformed), current smoking, current drinking, and use of lipid-lowering medications.
† Further adjusted for CETP D442G mutation.
CI = 95% confidence interval; OR = odds ratio; Q = quartile.

Table 3
Age and multivariate-adjusted associations of serum cholesteryl ester transfer protein (CETP) levels with intima-media thickness of common carotid artery in 250 Japanese men aged 40 to 49 years, Kusatsu City, Shiga, Japan, 2002–2004

Variable	CETP Quartiles				p for Trend
	Q1 (≤1.9; n = 56)	Q2 (2.0–2.1; n = 56)	Q3 (2.2–2.5; n = 73)	Q4 (≥2.6; n = 65)	
Age adjusted	602 (10)	616 (10)	619 (9)	641 (9)	0.05
Multivariate adjusted					
Model 1*	602 (10)	616 (10)	615 (9)	646 (9)	0.01
Model 2†	600 (10)	616 (10)	617 (9)	646 (9)	0.01

Data in parenthesis are standard errors.
* Adjusted for age, body mass index, hypertension, diabetes, triglycerides (log-transformed), current smoking, current drinking, and lipid-lowering medication use.
† Further adjusted for CETP D442G mutation.
CETP = cholesteryl ester transfer protein; Q = quartile.

best image for scoring and then measured the average IMT across 1-cm segments of the near and far walls of the common carotid arteries and the far wall of the carotid bulb and internal carotid arteries on both sides. The readers were unaware of the participant's characteristics and the study center. The correlation coefficient of the IMT between the sonographers and between the readers was 0.96 and 0.99, respectively.[12]

The Statistical Package for Social Sciences, version 14.0J (SPSS Japan, Tokyo, Japan) was used for statistical analysis. For a comparison of the risk factors across the CETP quartiles, tests for trend were done using generalized linear models and chi-square tests. Fisher's exact test was used to compare frequencies for medication. Logistic regression analyses were used to examine the contribution of serum CETP to CAC with adjustment for age, and further adjustment for body mass index, hypertension, diabetes, TG (log-transformed), current smoking, current drinking, and using lipid lowering medication (model 1) with additional adjustment for CETP D442G variant (model 2). General linear model analyses were used to examine the contribution of serum CETP to IMT. All probability values were 2-tailed, and all confidence intervals were estimated at the 95% level.

Results

The range of serum CETP was 1.1 to 4.2 mg/L. The mean value of serum CETP was 2.26 ± 0.45. Of the 250 participants, 14 were heterozygous for the CETP D442G missense variant (5.6%) and no homozygotes. The mean CETP level was significantly lower in those with participants than in those without the D442G variant: 1.79 ± 0.56 and 2.29 ± 0.43 mg/L, respectively ($p < 0.01$).

Table 1 lists the cardiovascular risk characteristics for the participants in each CETP quartile. Among the characteristics, the LDL cholesterol levels increased with an increasing concentration of CETP and the HDL cholesterol levels decreased with increasing CETP. The prevalence of the metabolic syndrome was almost similar in each CETP quartile. The mean IMT of the common carotid arteries was greater in the higher CETP quartiles. The prevalence of CAC showed a positive relation with the CETP quartile. The prevalence of the D442G missense variant was greatest in the lowest CETP quartile.

Table 2 lists the age-adjusted and multivariate-adjusted odd ratios for CAC in which comparisons were made between the top 3 CETP quartiles and the bottom quartile as a reference. The odds ratio for CAC in the highest CETP quartile was about 3 to 4 times greater than that in the bottom quartiles in all models.

Table 3 lists the age-adjusted and multivariate-adjusted IMT of the common carotid arteries among the CETP quartiles. In all models, the IMT of the common carotid arteries was positively associated with increasing serum CETP. Similar patterns were also observed when we used the average IMT of the whole or part of the carotid artery

(common carotid arteries or internal carotid artery and bulb), or when we excluded participants with plaque (data not shown).

Similar results were observed among those with normal (<1.7 mmol/L, 150 mg/dl, n = 148) and high TG levels (≥1.7 mmol/L, n = 102). The odds ratio for CAC with a 1-mg/L increase of serum CETP was 2.35 (95% confidence interval 0.52 to 10.6) in the normal TG group and 4.05 (95% confidence interval 1.05 to 15.7) in the high TG group (model 2). The serum CETP quartiles were also positively associated with the IMT of the common carotid arteries in both the normal TG group (model 2, adjusted mean 589, 606, 624, and 634 μm, p = 0.09) and the high TG group (model 2, adjusted mean 603, 636, 615, and 659 μm, p = 0.04).

No significant difference was found in the prevalence of CAC between participants with and without the CETP D442G variant (14.3% and 12.3%, respectively, p = 0.69). The age-adjusted IMT of the common carotid arteries was also similar in participants with and without the D442G variant (619 μm [SE 21] and 620 μm [SE 5], respectively; p = 0.94).

Discussion

This is the first community-based study to investigate the relation between serum CETP levels and subclinical atherosclerosis in Japan. The serum CETP levels in middle-age Japanese men were positively associated with CAC and IMT, independent of the presence of the CETP D442G missense variant. Furthermore, the increase in CAC prevalence and IMT seemed to be evident between the third and fourth (highest) quartile, at a CETP level of 2.6 mg/L.

The relation between the blood CETP levels and atherosclerosis is controversial. CETP transfers cholesteryl esters from antiatherogenic HDL cholesterol classes toward proatherogenic lipoproteins of lower density classes in exchange for TG.[1,13] Thus, a high transfer of cholesteryl esters from HDL to apolipoprotein B-containing lipoproteins might be involved in the development of atherosclerosis. Alternatively, CETP could inhibit atherosclerosis by accelerating the rate of reverse cholesterol transport, by which excess cholesterol in peripheral tissues is finally transported to the liver by way of the low-density lipoprotein receptor.[13,14]

Plasma CETP mass was associated with incident CHD in healthy participants in a United Kingdom community-based population, especially with high serum TG.[15] Another study showed a positive correlation between the plasma CETP concentration and carotid artery IMT.[16] CETP concentrations were significantly greater in 117 survivors of myocardial infarction and 110 patients with stroke compared to 335 healthy controls in Chinese subjects.[17] In middle-age men with CHD, high CETP levels were associated with faster progression of coronary atherosclerosis.[18] However, Colhoun et al[19] did not find any support for the hypothesis that increased plasma CETP activity levels were atherogenic in type 1 diabetic and nondiabetic controls using CAC as a measure of coronary atherosclerosis in a United Kingdom sample. de Vries et al[20] also suggested that no independent relation existed between the plasma CETP mass and IMT in type 2 diabetic and nondiabetic controls in a Dutch sample.

A recent clinical trial of the CETP inhibitor torcetrapib combined with atorvastatin was terminated because of excess deaths in the intervention group.[21] Torcetrapib treatment produced a substantial increase in HDL cholesterol and decrease in LDL cholesterol; however, it was also associated with an increase in blood pressure. Similar results were observed in other clinical trials targeting coronary atherosclerosis measured by ultrasonography[22] and increases in the maximum IMT.[23,24] No epidemiologic study has indicated a blood pressure increase in participants with genetic CETP mutations.[4,25-27] Furthermore, a recent analysis showed that regression of coronary atherosclerosis by torcetrapib was at least observed in the top quartile of HDL cholesterol change.[28] We believe more evidence from observational epidemiologic studies might help to better understand these results.

In the present study, we focused on the common CETP D442G gene variant. In epidemiologic studies of the CETP gene variants in Japanese and Japanese Americans, a relation between the CETP genotype, mainly the D442G gene variant, and CHD was not consistently observed.[4,25-27] Only 1 prospective study[25] showed a low risk of CHD in participants with high HDL cholesterol (≥60 mg/dl) in Japanese descendants in Hawaii, irrespective of their CETP genotype. The results of this prospective study were consistent with ours.

The present study had some limitations. The study was cross-sectional and, as such, could not prove a causal relation. Second, the blood CETP concentration is not always consistent with CETP activity, because a positive interaction exists between the plasma CETP concentration and TG on plasma cholesteryl ester transport, which underscores the contribution of the plasma CETP concentration.[1] However, the plasma CETP level itself also affects cholesteryl ester transport,[20] and some studies have indicated that the CETP concentration is strongly correlated with CETP activity.[29] We observed similar results in those with normal TG and high TG in the present study. Third, we did not test for other CETP gene variants. Fourth, with a relatively small sample size, it was difficult to compare the men with and without the D442G variant. Fifth, residual confounding factors might have been present such as socioenvironmental and behavioral factors. Finally, a study confided to men aged 40 to 49 might limit the generalization of the results to older men and women.

1. Tall AR. Plasma cholesteryl ester transfer protein. *J Lipid Res* 1993; 34:1255–1274.
2. Rumana N, Kita Y, Turin TC, Murakami Y, Sugihara H, Morita Y, Tomioka N, Okayama A, Nakamura Y, Ueshima H. Seasonal pattern of incidence and case fatality of acute myocardial infarction in a Japanese population (from the Takashima AMI Registry, 1988–2003). *Am J Cardiol* 2008;102:1307–1311.
3. Okamura T, Kokubo Y, Watanabe M, Higashiyama A, Miyamoto Y, Yoshimasa Y, Okayama A. Low-density lipoprotein cholesterol and non-high-density lipoprotein cholesterol and the incidence of cardiovascular disease in an urban Japanese cohort study: the Suita study. *Atherosclerosis* 2009;203:587–592.
4. Inazu A, Jiang XC, Haraki T, Yagi K, Kamon N, Koizumi J, Mabuchi H, Takeda R, Takata K, Moriyama Y, Doi M. Genetic cholesteryl ester transfer protein deficiency caused by two prevalent mutations as a

major determinant of increased levels of high density lipoprotein cholesterol. *J Clin Invest* 1994;94:1872–1882.
5. Sekikawa A, Ueshima H, Kadowaki T, El-Saed A, Okamura T, Takamiya T, Kashiwagi A, Edmundowicz D, Murata K, Sutton-Tyrrell K, Maegawa H, Evans RW, Kita Y, Kuller LH. Less subclinical atherosclerosis in Japanese men in Japan than in white men in the United States in the post-World War II birth cohort. *Am J Epidemiol* 2007; 165:617–624.
6. Okamura T, Kadowaki T, Sekikawa A, Murata K, Miyamatsu N, Nakamura Y, El-Saed A, Kashiwagi A, Maegawa H, Nishio Y, Takamiya T, Kanda H, Mitsunami K, Kita Y, Edmundowicz D, Tamaki S, Tsujita Y, Kuller LH, Ueshima H. Alcohol consumption and coronary artery calcium in middle-aged Japanese men. *Am J Cardiol* 2006;98: 141–144.
7. Nakamura Y, Ueno Y, Tamaki S, Kadowaki T, Okamura T, Kita Y, Miyamatsu N, Sekikawa A, Takamiya T, El-Saed A, Sutton-Tyrrell K, Ueshima H. Fish consumption and early atherosclerosis in middle-aged men. *Metabolism* 2007;56:1060–1064.
8. Sekikawa A, Curb JD, Ueshima H, El-Saed A, Kadowaki T, Abbott RD, Evans RW, Rodriguez BL, Okamura T, Sutton-Tyrrell K, Nakamura Y, Masaki K, Edmundowicz D, Kashiwagi A, Willcox BJ, Takamiya T, Mitsunami K, Seto TB, Murata K, White RL, Kuller LH; ERA JUMP (Electron-Beam Tomography, Risk Factor Assessment Among Japanese and U.S. Men in the Post-World War II Birth Cohort) Study Group. Marine-derived n-3 fatty acids and atherosclerosis in Japanese, Japanese Americans, and whites: a cross-sectional study. *J Am Coll Cardiol* 2008;52:417–424.
9. Sasai K, Okumura-Noji K, Hibino T, Ikeuchi R, Sakuma N, Fujinami T, Yokoyama S. Human cholesteryl ester transfer protein measured by enzyme-linked immunosorbent assay with two monoclonal antibodies against rabbit cholesteryl ester transfer protein: plasma cholesteryl ester transfer protein and lipoproteins among Japanese hypercholesterolemic patients. *Clin Chem* 1998;44:1466–1473.
10. Kokubo Y, Okamura T, Yoshimasa Y, Miyamoto Y, Kawanishi K, Kotani Y, Okayama A, Tomoike H. Impact of metabolic syndrome components on the incidence of cardiovascular disease in a general urban Japanese population: the Suita study. *Hypertens Res* 2008;31: 2027–2035.
11. Agatston AS, Janowitz WR, Hildner FJ, Zusmer NR, Viamonte M Jr, Detrano R. Quantification of coronary artery calcium using ultrafast computed tomography. *J Am Coll Cardiol* 1990;15:827–832.
12. Thompson T, Sutton-Tyrrell K, Wildman R. Continuous quality assessment programs can improve carotid duplex scan quality. *J vasc Technol* 2001;25:33–39.
13. Barter PJ, Brewer HB Jr, Chapman MJ, Hennekens CH, Rader DJ, Tall AR. Cholesteryl ester transfer protein: a novel target for raising HDL and inhibiting atherosclerosis. *Arterioscler Thromb Vasc Biol* 2003; 23:160–167.
14. Hirano K, Yamashita S, Nakajima N, Arai T, Maruyama T, Yoshida Y, Ishigami M, Sakai N, Kameda-Takemura K, Matsuzawa Y. Genetic cholesteryl ester transfer protein deficiency is extremely frequent in the Omagari area of Japan: marked hyperalphalipoproteinemia caused by CETP gene mutation is not associated with longevity. *Arterioscler Thromb Vasc Biol* 1997;17:1053–1059.
15. Boekholdt SM, Kuivenhoven JA, Wareham NJ, Peters RJ, Jukema JW, Luben R, Bingham SA, Day NE, Kastelein JJ, Khaw KT. Plasma levels of cholesteryl ester transfer protein and the risk of future coronary artery disease in apparently healthy men and women: the prospective EPIC (European Prospective Investigation into Cancer and nutrition)-Norfolk population study. *Circulation* 2004;110:1418–1423.
16. Föger B, Luef G, Ritsch A, Schmidauer C, Doblinger A, Lechleitner M, Aichner F, Patsch JR. Relationship of high-density lipoprotein subfractions and cholesteryl ester transfer protein in plasma to carotid artery wall thickness. *J Mol Med* 1995;73:369–372.
17. Zhuang Y, Wang J, Qiang H, Li Y, Lui X, Li L, Chen G. Serum cholesteryl ester transfer protein concentrations in healthy Chinese subjects and cardio-cerebrovascular disease patients. *Clinica Chim Acta* 2001;305:19–25.
18. Klerkx AH, de Grooth GJ, Zwinderman AH, Jukema JW, Kuivenhoven JA, Kastelein JJ. Cholesteryl ester transfer protein concentration is associated with progression of atherosclerosis and response to pravastatin in men with coronary artery disease (REGRESS). *Eur J Clin Invest* 2004;34:21–28.
19. Colhoun HM, Scheek LM, Rubens MB, Van Gent T, Underwood SR, Fuller JH, Van Tol A. Lipid transfer protein activities in type 1 diabetic patients without renal failure and nondiabetic control subjects and their association with coronary artery calcification. *Diabetes* 2001;50:652–659.
20. de Vries R, Perton FG, Dallinga-Thie GM, van Roon AM, Wolffenbuttel BH, van Tol A, Dullaart RP. Plasma cholesteryl ester transfer is a determinant of intima-media thickness in type 2 diabetic and nondiabetic subjects: role of CETP and triglycerides. *Diabetes* 2005;54: 3554–2559.
21. Barter PJ, Caulfield M, Eriksson M, Grundy SM, Kastelein JJ, Komajda M, Lopez-Sendon J, Mosca L, Tardif JC, Waters DD, Shear CL, Revkin JH, Buhr KA, Fisher MR, Tall AR, Brewer B; ILLUMINATE Investigators. Effects of torcetrapib in patients at high risk for coronary events. *N Engl J Med* 2007;357:2109–2122.
22. Nissen SE, Tardif JC, Nicholls SJ, Revkin JH, Shear CL, Duggan WT, Ruzyllo W, Bachinsky WB, Lasala GP, Tuzcu EM; ILLUSTRATE Investigators. Effect of torcetrapib on the progression of coronary atherosclerosis. *N Engl J Med* 2007;356:1304–1316.
23. Bots ML, Visseren FL, Evans GW, Riley WA, Revkin JH, Tegeler CH, Shear CL, Duggan WT, Vicari RM, Grobbee DE, Kastelein JJ; RADIANCE 2 Investigators. Torcetrapib and carotid intima-media thickness in mixed dyslipidaemia (RADIANCE 2 study): a randomised, double-blind trial. *Lancet* 2007;370:153–160.
24. Vergeer M, Bots ML, van Leuven SI, Basart DC, Sijbrands EJ, Evans GW, Grobbee DE, Visseren FL, Stalenhoef AF, Stroes ES, Kastelein JJ. Cholesteryl ester transfer protein inhibitor torcetrapib and off-target toxicity: a pooled analysis of the rating atherosclerotic disease change by imaging with a new CETP inhibitor (RADIANCE) trials. *Circulation* 2008;118:2515–2522.
25. Curb JD, Abbott RD, Rodriguez BL, Masaki K, Chen R, Sharp DS, Tall AR. A prospective study of HDL-C and cholesteryl ester transfer protein gene mutations and the risk of coronary heart disease in the elderly. *J Lipid Res* 2004;45:948–953.
26. Hirano K, Yamashita S, Nakajima N, Arai T, Maruyama T, Yoshida Y, Ishigami M, Sakai N, Kameda-Takemura K, Matsuzawa Y. Genetic cholesteryl ester transfer protein deficiency is extremely frequent in the Omagari area of Japan: marked hyperalphalipoproteinemia caused by CETP gene mutation is not associated with longevity. *Arterioscler Thromb Vasc Biol* 1997;17:1053–1059.
27. Moriyama Y, Okamura T, Inazu A, Doi M, Iso H, Mouri Y, Ishikawa Y, Suzuki H, Iida M, Koizumi J, Mabuchi H, Komachi Y. A low prevalence of coronary heart disease among subjects with increased high-density lipoprotein cholesterol levels, including those with plasma cholesteryl ester transfer protein deficiency. *Prev Med* 1998; 27(5 Pt 1):659–667.
28. Nicholls SJ, Tuzcu EM, Brennan DM, Tardif JC, Nissen SE. Cholesteryl ester transfer protein inhibition, high-density lipoprotein raising, and progression of coronary atherosclerosis: insights from ILLUSTRATE (Investigation of Lipid Level Management Using Coronary Ultrasound to Assess Reduction of Atherosclerosis by CETP Inhibition and HDL Elevation). *Circulation* 2008;118:2506–2514.
29. van Venrooij FV, Stolk RP, Banga JD, Sijmonsma TP, van Tol A, Erkelens DW, Dallinga-Thie GM; DALI Study Group. Common cholesteryl ester transfer protein gene polymorphisms and the effect of atorvastatin therapy in type 2 diabetes. *Diabetes Care* 2003;26:1216–1223.

Long-Term Prognosis of Probands With Brugada-Pattern ST-Elevation in Leads V_1–V_3

Shiro Kamakura, MD, PhD; Tohru Ohe, MD, PhD; Kiyoshi Nakazawa, MD, PhD; Yoshifusa Aizawa, MD, PhD; Akihiko Shimizu, MD, PhD; Minoru Horie, MD, PhD; Satoshi Ogawa, MD, PhD; Ken Okumura, MD, PhD; Kazufumi Tsuchihashi, MD, PhD; Kaoru Sugi, MD, PhD; Naomasa Makita, MD, PhD; Nobuhisa Hagiwara, MD, PhD; Hiroshi Inoue, MD, PhD; Hirotsugu Atarashi, MD, PhD; Naohiko Aihara, MD; Wataru Shimizu, MD, PhD; Takashi Kurita, MD, PhD; Kazuhiro Suyama, MD, PhD; Takashi Noda, MD, PhD; Kazuhiro Satomi, MD, PhD; Hideo Okamura, MD; Hitonobu Tomoike, MD, PhD; for the Brugada Syndrome Investigators in Japan

Background—The prognosis of patients with saddleback or noncoved type (non–type 1) ST-elevation in Brugada syndrome is unknown. The purpose of this study was to clarify the long-term prognosis of probands with non–type 1 ECG and those with coved (type 1) Brugada-pattern ECG.

Methods and Results—A total of 330 (123 symptomatic, 207 asymptomatic) probands with a coved or saddleback ST-elevation ≥1 mm in leads V_1–V_3 were divided into 2 ECG groups—type 1 (245 probands) and non–type 1 (85 probands)—and were prospectively followed for 48.7±15.0 months. The absence of type 1 ECG was confirmed by drug provocation test and multiple recordings. The ratio of individuals with a family history of sudden cardiac death (14%) was lower than previous studies. Clinical profiles and outcomes were not notably different between the 2 groups (annual arrhythmic event rate of probands with ventricular fibrillation; type 1: 10.2%, non–type 1: 10.6%, probands with syncope; type 1: 0.6%, non–type 1: 1.2%, and asymptomatic probands; type 1: 0.5%, non–type 1: 0%). Family history of sudden cardiac death at age <45 years and coexistence of inferolateral early repolarization with Brugada-pattern ECG were independent predictors of fatal arrhythmic events (hazard ratio, 3.28; 95% confidence interval, 1.42 to 7.60; P=0.005; hazard ratio, 2.66; 95% confidence interval, 1.06 to 6.71; P=0.03, respectively, by multivariate analysis), although spontaneous type 1 ECG and ventricular fibrillation inducibility by electrophysiological study were not reliable parameters.

Conclusions—The long-term prognosis of probands in non–type 1 group was similar to that of type 1 group. Family history of sudden cardiac death and the presence of early repolarization were predictors of poor outcome in this study, which included only probands with Brugada-pattern ST-elevation. (***Circ Arrhythmia Electrophysiol.* 2009;2:495-503.)**

Key Words: death, sudden ■ prognosis ■ follow-up studies ■ electrocardiography ■ Brugada syndrome

Brugada syndrome is a hereditary arrhythmogenic disease characterized by ST-elevation in the right precordial lead of standard ECGs and an increased risk of sudden cardiac death (SCD).[1] The prognosis for this condition and the management approaches have been reported in several multicenter studies of patients with the coved type 1 ECG. However, no prospective data have been reported in patients with saddleback type or noncoved Brugada-pattern ST-elevation before, because they were excluded from previous

Clinical Perspective on p 503

studies as atypical Brugada patients showing a benign clinical course. Besides, the data from previous studies are all conflicting with regard to the prognosis of the typical Bru-

Received August 22, 2008; accepted July 14, 2009.

From the Division of Cardiology (S.K., N.A., W.S., T.K., K.S., T.N., K.S., H.O., H.T.), National Cardiovascular Center, Suita, Japan; the Department of Cardiovascular Medicine (T.O.), Okayama University Graduate School of Medicine, Okayama, Japan; the Department of Cardiology (K.N.), St Marianna University, Kawasaki, Japan; the Division of Cardiology (Y.A.), Niigata University Graduate School of Medical and Dental Sciences, Niigata, Japan; the Division of Cardiology (A.S.), Yamaguchi University Graduate School of Medicine, Ube, Japan; the Department of Cardiovascular Medicine (M.H.), Shiga University of Medical Science, Otsu, Japan; the Department of Cardiopulmonary Medicine (S.O.), Keio University, Tokyo, Japan; the Second Department of Internal Medicine (K.O.), Hirosaki University School of Medicine, Hirosaki, Japan; the Second Department of Internal Medicine (K.T.), Sapporo Medical University School of Medicine, Sapporo, Japan; the Division of Cardiovascular Medicine (K.S.), Toho University Medical Center Ohashi Hospital, Tokyo, Japan; the Department of Cardiovascular Medicine (N.M.), Hokkaido University Graduate School of Medicine, Sapporo, Japan; the Department of Cardiology (N.H.), Tokyo Women's Medical University; the Second Department of Internal Medicine (H.I.), Toyama University, Toyama, Japan; and the Department of Internal Medicine, Nippon Medical School, Tama-Nagayama Hospital, Tokyo, Japan.

Correspondence to Shiro Kamakura, MD, PhD, Division of Cardiology, Department of Internal Medicine, National Cardiovascular Center, 5-7-1 Fujishiro-dai, Suita, Osaka, 565-8565, Japan. E-mail kamakura@hsp.ncvc.go.jp

Circ Arrhythmia Electrophysiol **is available at http://circep.ahajournals.org** **DOI: 10.1161/CIRCEP.108.816892**

gada syndrome.[2-5] This may be caused by cohort studies that included a significant number of family members other than probands, in which the prognosis of pedigree members can be affected by the disease severity of probands. Furthermore, a selection bias can be present if the data are analyzed retrospectively. Therefore, we aimed to investigate the long-term prognosis of probands with noncoved type ST-elevation in leads V_1–V_3, prospectively, and compared it with that of probands with the type 1 ST-elevation.

Methods

Patient Population

A total of 330 individuals with spontaneous ST-elevation were registered consecutively in this study, namely, "a multicenter study for risk stratification and management in patients with Brugada syndrome." The study was conducted at 26 institutions across Japan beginning in July 2001. These individuals were prospectively followed up for more than 12 months to the end of March 2007. Subjects were enrolled in this study if they met the following inclusion criteria: (1) proband, (2) J-point (QRS-ST junction) amplitude of ≥0.1 mV (1 mm) with either coved or saddle back type ST-segment elevation in at least 2 of the 3 precordial leads (V_1–V_3) on resting standard 12-lead ECG, (3) normal findings on physical examination, and (4) no abnormality in either right or left ventricular morphology and/or function demonstrated by chest radiography and echocardiography. Patients with vasospastic angina and those with vasovagal syncope were excluded from this study. Patients were not administered antiarrhythmic drugs and did not have electrolyte abnormalities at the time of baseline ECG recording and other examinations.

Classification of Groups

We divided the 330 patients with Brugada-pattern ECG into 3 groups according to their symptoms: The ventricular fibrillation (VF) group consisted of 56 probands with aborted sudden death and/or documented VF, the syncope group consisted of 67 probands with syncope without documented arrhythmias that was not typical for vasovagal syncope, and the asymptomatic group consisted of 207 asymptomatic individuals whose ECGs were mainly detected by individual annual medical checkup or health screening in their place of employment.

We also divided these patients into 2 groups according to ECG morphology: The type 1 group consisted of 245 probands with a spontaneous type 1 ECG or those who developed type 1 ECG with a drug provocation test. The non–type 1 group consisted of the remaining 85 probands who never showed type 1 ST-elevation even with the drug provocation test (Figure 1) and during the follow-up on standard 12-lead ECGs.

Clinical Data, ECG, and Electrophysiological Testing

Clinical data including age at the enrollment, sex, family history of SCD, and the presence of atrial fibrillation were collected for all patients. The standard ECGs were recorded more than 5 times during the follow-up period in all patients. ECG recording on higher intercostals spaces (third and/or second) in leads V_1–V_3[6] was encouraged in patients who had cardiac events during the follow-up period.

A type 1 ECG was defined as a prominent coved ST-segment elevation displaying J-point wave amplitude or ST-segment elevation ≥2 mm or 0.2 mV.[7,8] ECG patterns with a prominent coved ST-elevation ≥2 mm followed by a positive or flat T wave were also included in type 1 group (Figure 2A through C). A non–type 1 ECG was defined as one of the following: type 2 ECG,[7] type 3 ECG,[7] and ECG displaying coved or saddleback ST-elevation with J-wave amplitude ≥1 mm and <2 mm (Figures 1 and 2D through 2G).

The presence of early repolarization in the inferolateral leads[9] was evaluated by baseline 12-lead ECGs at the time of enrollment to elucidate ECG findings associated with Brugada syndrome. Early repolarization was defined as an elevation of the J point in at least 2 leads. The amplitude of the J wave or J-point elevation had to be at least 1 mm above the baseline level, either as QRS slurring or notching in the inferior lead (II, III, and aVF), lateral (I, aVL, and V_4–V_6) lead, or both.[9]

ECGs were evaluated by 3 independent investigators (S.K., N.A., and W.S.) who were unaware of the patients' other clinical information. The ECG type or morphology was established by the evaluation in which at least 2 of the 3 observers were in agreement.

Sodium channel blocker pilsicainide (1 mg/kg body weight at a rate of 5 to 10 mg/min), disopyramide (1.5 mg/kg, 10 mg/min), flecainide (2 mg/kg, 10 mg/min), or procainamide (10 mg/kg, 100 mg/min) was administered intravenously in 270 (82%) patients (233, 15, 14, and 8, respectively) to test the conversion to typical coved ST-elevation.[8,10,11]

Baseline electrophysiological studies (EPS) were performed in 232 (70%) patients. A maximum of 3 ventricular extrastimuli were delivered from 2 right ventricular (RV) sites (RV apex and RV outflow tract) unless VF or polymorphic ventricular tachycardia (VT) (lasting ≥10 beats) that terminated spontaneously within 30 seconds, causing syncope, or requiring intervention to be terminated was elicited at a previous step. Premature beats were started in late diastole; coupling intervals were then reduced in 10-ms decrements until refractoriness was reached. Stimulation was performed at twice the diastolic threshold. Patients with inducible ventricular arrhythmias lasting less than 10 beats were classified as noninducible. The indices including age, sex distribution, a family history of SCD at

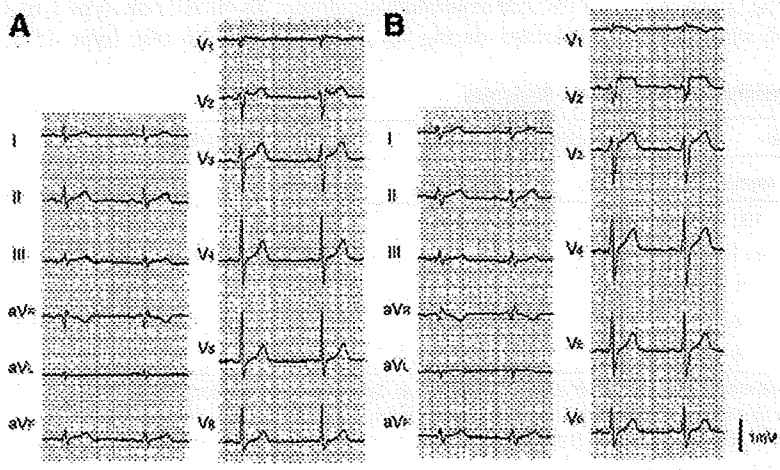

Figure 1. Presentation of 12-lead ECGs of a patient with non–type 1 ST-elevation. A, Baseline 12-lead ECG; B, 12-lead ECG after provocation by intravenous administration of 50 mg pilsicainide in the same patient. Saddleback-type ST-elevation in leads V_1 and V_2 was enhanced after pilsicainide but was not changed to type 1 ST-elevation. This 46-year-old male patient with a history of syncope but with no family history of SCD had inducible VF by electrophysiological study. He had spontaneous VF 11 months after enrollment.

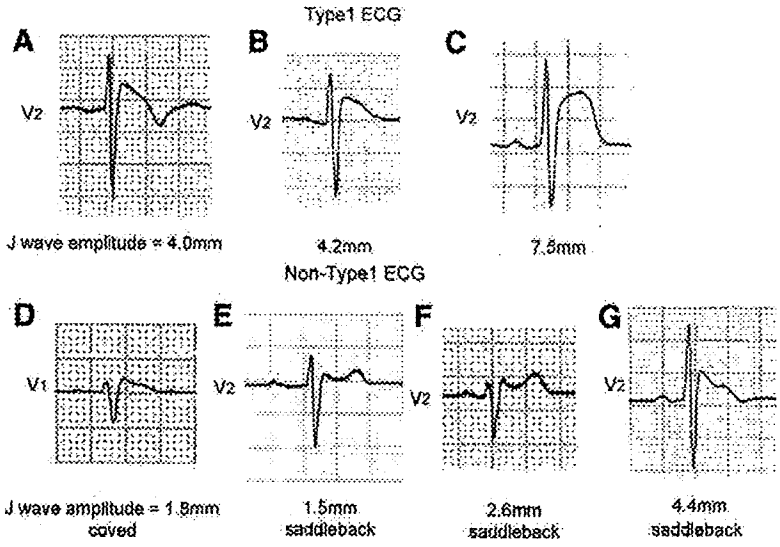

Figure 2. Presentation of type 1 and non–type 1 ECG. Coved-type ST-elevation with a J-wave amplitude ≥2 mm followed by a negative T wave (A) or a positive/flat T wave (B), and a coved ST-elevation followed by a smaller J wave than T wave (C) were defined as type 1 ECG. Coved (D) or saddleback-type ST-elevation (E) with a J-wave amplitude <2 mm, a saddleback ST-elevation with a J-wave amplitude ≥2 mm (F), and a saddleback ST-elevation displaying bigger J wave than T wave (G) were defined as non–type 1 ECG.

less than 45 years of age, and VF/polymorphic VT inducibility were compared with those reported in previously published studies[2,3,5] (Table 1). In addition to these parameters, the presence of atrial fibrillation, cardiac events at night, and inferolateral early repolarization were compared between type 1 and non–type 1 groups.

Patient treatment was based on clinical judgment of the participating hospital. Twenty-eight (8%) probands received antiarrhythmic drugs (quinidine sulfate ≤400 mg, bepridil ≤200 mg, disopyramide ≤300 mg, aprindine ≤30 mg, and amiodarone ≤200 mg/d) for prevention of atrial fibrillation or VF. Calcium antagonists were administered in 18 (5%) probands for hypertension. Quinidine and bepridil were administered only after a documentation of VF during follow-up. Among the 330 patients, 125 (38%) received an implantable cardioverter-defibrillator (ICD). During follow-up, patients were considered to have an arrhythmic event if sudden death occurred or VF was documented.

Statistical Analysis

Data are presented as mean±standard deviation. The Fisher exact test or the χ^2 test was used for categorical variables. One-way ANOVA was used for comparisons of continuous variables among the different groups. Survival curves were plotted by the Kaplan-Meier method and analyzed by the log-rank test. Cox proportional hazards models were used to analyze factors associated with the time to the first arrhythmic event during follow-up in all probands as well as in type 1, non–type 1, VF, and non-VF (syncope and asymptomatic) groups. Variables were included in the multivariate analysis with the use of a forward stepwise procedure with a criteria of $P<0.05$ for inclusion and $P>0.15$ for removal from the model. A probability value of $P<0.05$ was considered statistically significant.

This study was performed under the ethical code approved by the Health, Labor, and Welfare Ministry of Japan. Written informed consent was obtained from all individuals.

Results

Clinical Profiles of All Probands

The mean age of the 330 probands was 51.4±14.8 years (median, 53 years; range, 4 to 86 years). The majority (315; 95%) of probands were male. A low percentage (14%) of patients had a family history of SCD occurring before the age of 45 years. The induction rate of VF/polymorphic VT by EPS was higher (77/109: 72%, $P<0.005$) in symptomatic than asymptomatic probands (61/123: 50%) (Table 1).

Comparison of Clinical Characteristics Between Type 1 and Non–Type 1 Groups

Type 1 ECG was found in 245 probands (VF group: 45, 18%; syncope group: 46, 19%; and asymptomatic group: 154, 63%). Of these 245 probands, 173 (71%) showed type 1 ECG spontaneously and the remaining 72 (29%) showed characteristic type 1 morphology after class Ic or Ia antiarrhythmic drug administration. In 85 probands of the non–type 1 group (VF group: 11, 13%; syncope group: 21, 25%; and asymptomatic group: 53, 62%), non–type 1 ECG remained during the drug provocation test (type 2: 61,

Table 1. Comparison of Patient Characteristics Among 3 Large Registries

	Brugada et al[2]		Eckardt et al[5]		Kamakura et al	
	Sympt	Asympt	Sympt	Asympt	Sympt (VF, S)	Asympt
No.	144	190	89	123	123 (56, 67)	207
Age, y	41±16*	40±16	46±14	44±14	50.4±16.6	51.9±13.6
Men, %	83	71	76	68	96	95
FH of SCD, %	34	72	21	33	19 (25, 13)	11
VF/VT inducibility, %	73	33	63	39	71 (65, 75)	50

Values in parentheses are for the patients with aborted sudden death and an episode of syncope. Sympt indicates symptomatic; Asympt, asymptomatic; S, syncope; FH of SCD, prevalence of patients with a family history of sudden cardiac death at <45 years old; and VF/VT inducibility, induction rate of VF or polymorphic ventricular tachycardia by EPS.

*Age of patients with VF.

Table 2. Comparison of Clinical Profiles Between Probands With Type 1 ECG and Those With Non–Type 1 ECG

	Type 1 (n=245)			Non-Type 1 (n=85)			
	VF	Syncope	Asympt	VF	Syncope	Asympt	*P* Value
No.	45	46	154	11	21	53	0.33
Age, y	48.2±17.8	52.5±15.6	52.3±13.1	48.0±18.1	51.9±15.8	50.7±15.2	0.99
Men, n (%)	44 (98)	44 (96)	146 (95)	11 (100)	19 (90)	51 (96)	0.90
FH of SCD, n (%)	11 (24)	8 (17)	17 (11)	3 (27)	1 (5)	5 (9)	0.06
Event at night, n (%)	37/45 (82)	15/45 (33)		5/9 (56)	7/18 (39)		0.06
Inferolateral ER, n (%)	8 (18)	3 (7)	15 (10)	2 (18)	1 (5)	4 (8)	0.85
Prevalence of AF, n (%)	19 (42)	7 (15)	21 (14)	4 (36)	3 (14)	8 (15)	0.87
VF/VT inducibility, n (%)	27/41 (66)	31/40 (78)	52/91 (57)	7/11 (64)	12/17 (71)	9/32 (28)	0.04

n (%) indicates the number and the ratio of patients with each parameter; event at night, event developed at night (8 PM to 8 AM); inferolateral ER, inferolateral early repolarization; AF, atrial fibrillation; VF/VT inducibility, induction rate of VF or polymorphic ventricular tachycardia by EPS.

72%; coved with J-point amplitude <2 mm: 24, 28%) and the follow-up period. Most of the clinical parameters except for VF/VT inducibility, namely, age, sex distribution, the prevalence of atrial fibrillation, the presence of a family history of SCD, cardiac events at night (8 PM to 8 AM), and early repolarization, were of similar occurrence between type 1 and non–type 1 groups (Table 2). Only 8% (7/85) of probands in the non–type 1 group and 11% (26/245) of those in the type 1 group were associated with early repolarization in the inferolateral leads.

Follow-Up and Predictors of Outcome

The mean follow-up period for the entire study population was 48.7±14.9 months. Follow-up time was similar among VF (51.9±15.0 months), syncope (48.5±14.0 months), and asymptomatic (47.7±15.0 months) groups and between type 1 (48.6±15.2 months) and non–type 1 (48.9±14.2 months) groups. Twenty-four patients had fatal arrhythmic events during follow-up. The frequency of events in the type 1 group—15 of 45 (33%) in patients with VF, 1 of 46 (2%) in syncope patients, and 3 of 154 (2%) in asymptomatic patients— was similar to that in the non–type 1 group (4/11: 36%, 1/21: 5%, and 0/53: 0%, respectively, $P=0.22$; Figure 3). In 5 patients who had events in the non–type 1 group, 2 had shown a type 1 ST-elevation only in the higher (second or third) intercostal spaces—1 in a follow-up ECG and 1 after drug provocation test. The observed frequency of arrhythmic events was significantly highly in patients with early repolarization in the inferolateral leads (7/33; 21% versus 17/297; 6%, $P<0.005$), although there was no difference in risk between the 2 groups (type 1: 6/26; 23%, non–type 1: 1/7; 14%, $P=0.67$). One asymptomatic patient with type 1 ECG died suddenly 3 months after enrollment. Six patients died of nonarrhythmic causes; 3 died of cancer, 1 because of rupture of abdominal aortic aneurysm, 1 because of pneumonia, and cause of death for 1 patient was unknown. Seven percent of all patients who entered the study dropped out, the most frequent reason for drop-out was inability of follow-up due to patient's change of address.

Figure 4 shows the Kaplan–Meier analysis of arrhythmic events in probands with type 1 and non–type 1 ECG. Probands in the VF group had significantly worse prognosis than those in the syncope and asymptomatic groups. The

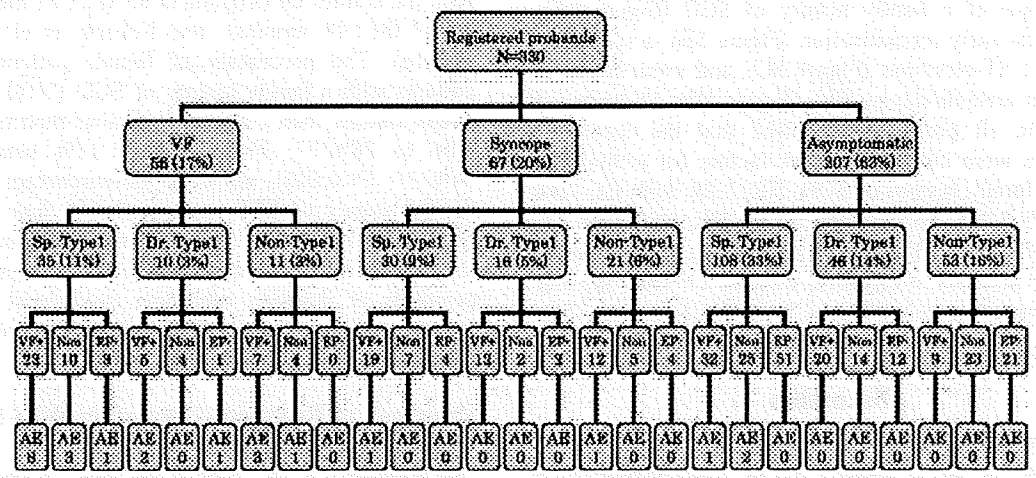

Figure 3. Flow chart of proband groups categorized according to symptom, ECG morphology, and VF/VT inducibility by electrophysiological study. Sp. Type 1 indicates spontaneous type 1 group; Dr. Type 1, drug-induced type 1 group; VF+, a group with inducible VF/VT; Non, a group with noninducible VF/VT; EP−, a group in which electrophysiological study was not performed; AE, fatal arrhythmic event during follow-up. The number indicates the number of probands in each category.